PERGAMON

Journal of Structural Geology 24 (2002) 57–76

JOURNAL OF STRUCTURAL GEOLOGY

www.elsevier.com/locate/jstrugeo

Modelling the bulk viscosity of two-phase mixtures in terms of clast shape

Susan H. Treagus*

Department of Earth Sciences, University of Manchester, Manchester M13 9PL, UK

Revised 26 February 2001; accepted 22 March 2001

Abstract

The rheological behaviour of many rock-types will depend on how mixtures of different minerals and rock clasts behave together. This paper develops two-dimensional modelling of the bulk viscosity of two-phase viscous mixtures with different shape fabrics in pure shearing, based on self consistent mechanics and behaviour of inclusion-matrix systems. An equation is presented for the bulk viscosity in terms of the phase viscosity contrast, phase fractions, and clast shape. Results are given for idealised two-dimensional mixtures of circles, squares or ellipses with a variety of phase viscosity contrasts, in pure shearing parallel/perpendicular to the shape fabric. The normalised bulk viscosities of all these mixtures fall between the theoretical upper and lower viscous bounds given by homogeneous strain-rate and homogeneous stress, respectively, but nearer to the upper bound with increasing shape fabric. Mixtures with a particular geometry are shown to have a constant 'relative horizontal distance' between these two bounds, as proposed by P.D. Bons.

Using graphs for the normalised bulk viscosities of mixtures with variably elliptical aligned shape fabrics, the results for fabrics orthogonal to pure shearing can be extrapolated to: (a) diagonal fabrics in pure shearing, and (b) orthogonal or diagonal fabrics in simple shearing. These reveal the bulk viscous anisotropy of mixtures with shape fabric, in two dimensions. It is speculated that during a progressive finite deformation, two-phase mixtures might undergo changes in bulk viscosity over time, with steady stiffening during pure shear, and perhaps cyclic stiffening and softening during simple shear. The two-dimensional models provide an approximation to the three-dimensional properties of mixtures with shape fabrics, with potential applications to rocks, including conglomerates.

Keywords: Bulk viscosity; Clast shape; Viscous mixtures; Two-phase composites

1. Introduction

1.1. Rocks and analogous mixtures, suspensions and composites

Most kinds of rocks are multiphase mixtures of clasts, grains or crystals, on some scale. Accordingly, it would be expected that their bulk rheological properties will, in part, be a function of the properties of the component phases. The present study has been prompted by attempts to express the bulk viscosity of an idealised conglomerate in terms of the viscosities of component clast and matrix phases, and their mutual relationships to strain: questions first considered by Gay (1968a,b). If such a rock mixture is simplified to just two phases, it has analogies with: (i) the elastic properties of two-phase composites in materials science (e.g. Hashin, 1983), (ii) the rheology of suspensions of one phase in another, from the field of applied rheology (e.g. Collyer and Clegg, 1988; Ferguson and Kemblowski, 1991), and (iii) the properties of two-phase mineral aggregates (e.g. Tullis et al., 1991; Bons, 1993; Handy, 1994; Takeda, 1998). Relevant theory and results from all these approaches will be reviewed in the following sections, and then used to develop simple theoretical modelling for idealised mixtures that can be applied to rocks with shape fabrics. The term *mixture* will be used, throughout, as a general term for aggregates, suspensions or composites comprising two or more different phases with definable geometry: it implies no mixing in the fluid sense (i.e. no miscibility).

1.2. Composites and their upper and lower elastic/viscous bounds

Hashin (1983) provides an informative and comprehensive review of elastic composite materials of varying kinds, which includes a discussion of 'variational bounds' for estimating or constraining the effective bulk elastic properties. The absolute theoretical upper and lower limits (bounds) for the bulk elastic moduli are determined by assuming either equal strain or equal stress in the two phases

* Tel.: +44-161-275-3804; fax: +44-161-275-3947.
E-mail address: s.treagus@man.ac.uk (S.H. Treagus).

0191-8141/02/$ - see front matter
PII: S0191-8141(01)00049-9

(Hill, 1965; Hashin, 1983). The same principles apply to a viscous composite or mixture, and the bounds on its bulk viscosity. Writing for a viscous two-phase mixture, the upper bound (subscripted U), sometimes termed the Voigt bound, is defined by assuming homogenous straining in the mixture, thus:

$$\mu_U = \alpha_1\mu_1 + \alpha_2\mu_2 \quad (1)$$

where μ_1 and μ_2 are the phase viscosities (Newtonian), and α_1 and α_2 are the phase fractions (with $\alpha_1 + \alpha_2 = 1$). μ_U varies linearly from μ_1 to μ_2, as α_2 changes from zero to one. The lower bound (subscripted L), sometimes termed the Reuss bound, is defined by assuming homogenous stress in the mixture:

$$\mu_L = 1/\{\alpha_1/\mu_1 + \alpha_2/\mu_2\} \quad (2)$$

μ_L varies nonlinearly from μ_1 to μ_2, with α_2 of zero to one. By definition, μ_U is always greater than μ_L.

For statistically isotropic composites or mixtures, these expressions bracket the permissible range within which the bulk viscosity must lie, and this range broadens with increasing phase viscosity contrast. It is interesting to note that Eqs. (1) and (2) have identical form to those for normal and shear viscosities (μ_n, μ_s) of a bilaminate multilayer, if considered as a statistically anisotropic material (Biot, 1965, pp. 186 and 432; Cobbold, 1976).

1.3. Statistically isotropic two-phase composites and self consistent mechanics (SCM)

Fundamental in the studies of composites reviewed by Hashin (1983) is that they are considered statistically isotropic materials with average (bulk) properties that can be defined in terms of the properties of the two phases. In a two-phase composite, the bulk stress (σ^*) and bulk natural strain (ε^*) are each defined as 'weighted averages' of the stresses and strains in phase 1 (σ_1, ε_1) and phase 2 (σ_2, ε_2) (Hill, 1965, eq. 8):

$$\sigma^* = \alpha_1\sigma_1 + \alpha_2\sigma_2 \quad (3)$$

$$\varepsilon^* = \alpha_1\varepsilon_1 + \alpha_2\varepsilon_2 \quad (4)$$

Writing Eq. (3) for linear viscous (Newtonian) materials, in terms of viscosities (μ_1, μ_2) and strain rates ($\dot{e}_1$, $\dot{e}_2$) gives:

$$\mu^*\dot{e}^* = \mu_1\alpha_1\dot{e}_1 + \mu_2\alpha_2\dot{e}_2 \quad (5)$$

This is more conveniently expressed over a small time increment, in terms of infinitesimal natural strains, ε:

$$\mu^*\varepsilon^* = \mu_1\alpha_1\varepsilon_1 + \mu_2\alpha_2\varepsilon_2 \quad (6)$$

Combining Eq. (6) with Eq. (4) leads to the following relationship for a viscous two-phase composite:

$$\mu^* = \mu_1 + \alpha_2(\mu_2 - \mu_1)(\varepsilon_2/\varepsilon^*) \quad (7)$$

(This expression could alternatively have been written in terms of $\varepsilon_1/\varepsilon^*$.)

Eq. (7) is the linear-viscous equivalent to the equation written for the shear moduli in elastic two-phase composites (Hashin, 1983, eq. 3.1.3). An expression for $(\varepsilon_2/\varepsilon^*)$ is needed in order to find a solution for the bulk mixture viscosity, μ^*.

This method of averaging underlies the *self consistent mechanics* (SCM) of composites, developed by Budiansky (1965) and Hill (1965) from even earlier studies of crystalline aggregates. Many decades later, the exact meaning of 'self consistent' may have become obscure. My interpretation is that all the grains of a particular phase are considered to behave self-consistently, undergoing the same stress and strain(-rate), and behaving as if each were in isolation in a statistically uniform surrounding medium. Hill (1965) considered the two-phase composite to be statistically isotropic, comprising a dispersed phase of spherical inclusions (here phase 2) in a continuous phase (phase 1). All the phase 2 inclusions deform homogeneously by the same strain, as 'isolated' inclusions in an 'effective matrix' that has the bulk composite properties. The bulk stress (σ^*) and bulk strain (ε^*) are taken as volume-weighted averages of the two phase stresses and strains, as given above (Eqs. (3) and (4)).

Hill (1965) obtained the required expression for $(\varepsilon_2/\varepsilon^*)$ for Eq. (7) from Eshelby's (1957) analysis of an isolated spherical inclusion in an infinite matrix. Written in Newtonian viscous nomenclature (after Eshelby, 1957; Bilby et al., 1975), the infinitesimal natural strain (ε_2) of an isolated spherical inclusion of viscosity μ_2, in coherent contact with a matrix that has the viscosity μ^*, undergoing bulk pure shearing in plane strain, with a strain given by ε^*, is:

$$\varepsilon_2/\varepsilon^* = 5/\{3 + 2(\mu_2/\mu^*)\} \quad (8)$$

Substituting this expression in Eq. (7) leads to a quadratic equation for the bulk viscosity (μ^*) of a statistically isotropic two-phase composite with a spherical clast fraction, in terms of phase viscosities and clast volume fraction (α_2):

$$3\mu^{*2} + \mu^*\{(2\mu_2 - 3\mu_1) - 5\alpha_2(\mu_2 - \mu_1)\} - 2\mu_1\mu_2 = 0 \quad (9)$$

If written in terms of both phase fractions (α_1, α_2), this becomes equivalent (by viscous correspondence) to the symmetrical expression derived by Hill (1965) for elastic composites:

$$3\mu^{*2} + \mu^*\{2(\mu_1 + \mu_2) - 5(\alpha_1\mu_1 + \alpha_2\mu_2)\} - 2\mu_1\mu_2 = 0 \quad (10)$$

The (real) solutions for μ^* have smoothly increasing values between the two end-member values of μ_1 and μ_2, as the fractions change. It can be shown that μ^* always falls between the upper and lower bounds defined above (Eqs. (1) and (2)), a first test of validity. The limiting case of $\mu_2/\mu_2 = \infty$ defines a suspension of rigid spherical inclusions of phase 2 in a viscous matrix of phase 1, and then Eq. (9) becomes:

$$\mu^*/\mu_1 = 1/\{1 - 2.5\alpha_2\} \quad (11)$$

This solution is limited to suspensions with $\alpha_2 < 0.4$. At $\alpha_2 = 0.4$ the mixture is defined as rigid.

If Eq. (11) is restricted to a very disperse suspension ($\alpha_2 < 0.1$), it can be approximated to:

$$\mu^*/\mu_1 = 1 + 2.5\alpha_2 \quad (12)$$

This equation, attributed to Einstein (1906), shows that a weak suspension of rigid spheres in a Newtonian fluid will behave as another linear fluid, with its 'relative viscosity' linearly related to the volume fraction.

Discussion and criticisms of this self consistent mechanics (SCM) approach focus on two aspects. First, because this method largely ignores interactions among the two phases, it has been argued (for elastic materials) that the analysis should be restricted to small volume fractions of either phase (Eshelby, 1957; Hill, 1965). Secondly, and related to this point, the inclusion boundary solution on which this SCM method is based satisfies requirements of continuity of stresses and strains in the inclusion, relative to the whole system. Or in the words of Hashin (1983), the SCM method 'assumes that a tree sees a forest—but a tree sees only other trees'. These reservations will also apply to the modelling of other viscous composites developed later in this paper. Nevertheless, this method arguably provides a better way to approximate the bulk properties of mixtures than using variational bounds.

The SCM analysis of Hill (1965) concentrated on treating the composite, statistically, in terms of a phase of spherical inclusions dispersed in a 'matrix phase' that is implied to be continuous. On the other hand, Budiansky (1965) applied similar SCM principles to multiphase materials envisaged as composites of irregular grains of two phases, whose shapes each do not deviate far from spherical. I prefer this latter definition for SCM modelling, for the following reasons. It is apparent from the symmetry in Eq. (10), that there is no real difference between 'particle' and 'matrix' phases (phases 2 and 1). The same result for μ^* would be found for $\alpha_1 = \alpha_2 = 0.5$ fractions, whichever phase is defined as stiffer, or whichever phase is considered 'spherical'. Hashin (1983) cited this as another criticism of SCM, stating that a stiff matrix should actually make a stiffer composite than a stiff particulate phase. However, the paradox is averted if the composite is imagined as a mixture of two spherical-grained phases. The validity of adopting this approach is also verified by applying Eshelby's relationship (Eq. (8)) for both phases (i.e. writing for $\varepsilon_1/\varepsilon^*$ and $\varepsilon_2/\varepsilon^*$), and using both in the strain averaging function (Eq. (4)). This produces exactly the same expression for μ^* as given in Eq. (10), and does not directly use the average stress expressions (Eqs. (3), (5) and (6)). This approach and method will therefore be applied in the two-dimensional modelling developed later, in Section 3.

1.4. Analogue and theoretical geological modelling

A number of laboratory-based studies and numerical methods have produced results for the bulk properties of two-phase aggregates of rock minerals or analogue materials, and examined the variations of stress, strain and strength with changing fractions of two granular phases. Jordan (1987) investigated the bulk strength of limestone–halite aggregates in the laboratory and applied the results more generally to the rheology of polymineralic rocks. Bloomfield and Covey-Crump (1993) studied a similar calcite–halite aggregate in the laboratory, up to 20% strain, with the aim of quantifying the aggregate stress and strain properties in terms of those of the two component phases. They found that the microstructural changes ensured that there was minimal strain partitioning between the two phases, and the aggregate properties fell close to the upper (Voigt) bound.

Tullis et al. (1991) approached the question of the rheology of mixtures by finite-element (FE) modelling. Based on Maryland diabase rock, these FE models have non-linear flow properties that simulate plagioclase and pyroxene, using laws derived from laboratory studies. The two-dimensional models are mainly square 'grains' of one phase, uniformly arranged in a matrix of the other phase, but a few models consider circular 'grains'. The bulk properties are shown to be dependent on strain-rate, as would be expected for mixtures of two power-law phases. However, they also reveal a dependence on the element 'grain' shape, with bulk properties for mixtures with square 'grains' falling closer to the upper bound than for the circular-grained models.

Ji and Zhao (1993) and Handy (1994) discuss more general aspects of flow laws from multiphase rocks, including discussion of texture and grain size. Ji and Zhao (1993) focus on methods of using experimental data to determine bulk flow properties in terms of the constituent phases. Handy (1994) takes a 'phenomenological' approach, focusing on non-linear phases and two-phase mixtures that are conceived to be in finite simple shear deformation, up to high strains where strong shape fabrics are expected to develop. He constructs a schematic 'structural stability diagram' for the rheology of a two-phase mixture of quartz (weak) and feldspar (strong). His results depend on assuming a 'strain-rate concentration function' in the weaker phase, that turns out to be similar to the strain-rate intensity factor derived by Treagus (1993) for incompetent layers in a bilaminate multilayer (with power-law rheology, and the same stress exponent) in layer-parallel simple shear. Handy's (1994) schematic curves for composite properties may thus simulate the bulk properties of strongly sheared mixtures with a foliation.

In a major study of the deformation of polyphase aggregates, Bons (1993) provides a comprehensive review of the subject, and new work in several areas. He takes an experimental approach using mixtures of analogue materials: camphor (strong) and octachloropropane (OCP; weak). This is accompanied by finite-element models of theoretical mixtures in two dimensions (Bons, 1993; Bons and Cox,

1994). Most of Bons's numerical models have elastic parameters and hexagonal elements to simulate grains, but some use Newtonian to power-law rheology, using square elements. Both FE model series were designed with 'grains' that are randomised strings of a number of elements of the same phase, and so the bulk rheology is partly a measure of this anisotropy. These models provide an important source for comparison with the theoretical modelling developed later in this paper. A significant conclusion of Bons and Cox (1994) is that the bulk viscosities of these FE model composites occupy a constant fractional position on a horizontal scale (of α_1 or α_2) between the upper- and lower-bound curves, for any given inclusion geometry. For isotropic mixtures, this constant 'relative horizontal distance' (which Bons terms H) is stated to be approximately 0.5: i.e. halfway horizontally between the upper and lower bounding curves. This result will be returned to later in the paper, and tested.

Takeda (1998) recently considered the theory of bulk flow of multiphase mixtures of different Newtonian fluids, including simplification to a two-phase system of the kind discussed here. His variables are the viscosities of the two phases and their densities, both normalised as ratios, and the phase fractions. Takeda produces a quadratic expression that has two solutions for the normalised bulk viscosity of two-phase mixtures, which he terms Modes 1 and 2. If there are no density contrasts, the Mode 1 and 2 solutions are equivalent to the upper and lower bounds, respectively (Eqs. (1) and (2)). This would imply that the bulk viscosity must have the value of either the upper or the lower bound, rather than a specific value in between, as will be sought for different types of mixtures in the present paper.

2. Two-dimensional strain of isolated inclusions in a matrix

2.1. Introduction to two-dimensional modelling

This paper aims to derive algebraic expressions for the bulk viscosity of two-phase viscous mixtures, in terms of the phase viscosities and their fractional concentrations, but including an additional property to describe particle or clast shape. The analysis will be two-dimensional, combining theory and modelling of strain of isolated inclusions of different shape, in a contrasting matrix. It is based on the same principles of self consistent mechanics (SCM) of composites as introduced in Section 1.3, which were described in terms of three-dimensional mixtures of spherical clasts. The role of clast geometry on mixture viscosity is easier to examine in two-dimensional analyses. As outlined in Section 1.3 (Eqs. (8)–(10)), the method is developed from theory and modelling of isolated inclusions in a matrix.

Two-dimensional modelling of inclusion-matrix systems focuses on circular or elliptical inclusions that should strictly be considered to be cross-sections of cylinders aligned in the third dimension of no strain (Eshelby, 1957; Bilby et al., 1975; Bilby and Kolbussewski, 1977). This 'cylinder' model also needs to be applied conceptually to finite element models of inclusion-matrix systems, such as the circular inclusions presented by Shimamoto (1975), and the square inclusions modelled by Treagus et al. (1996) and Treagus and Lan (2000). For simplicity from now on, all these inclusions will be referred to by their two-dimensional shape, as circular, elliptical, square etc. inclusions, as depicted in Fig. 1.

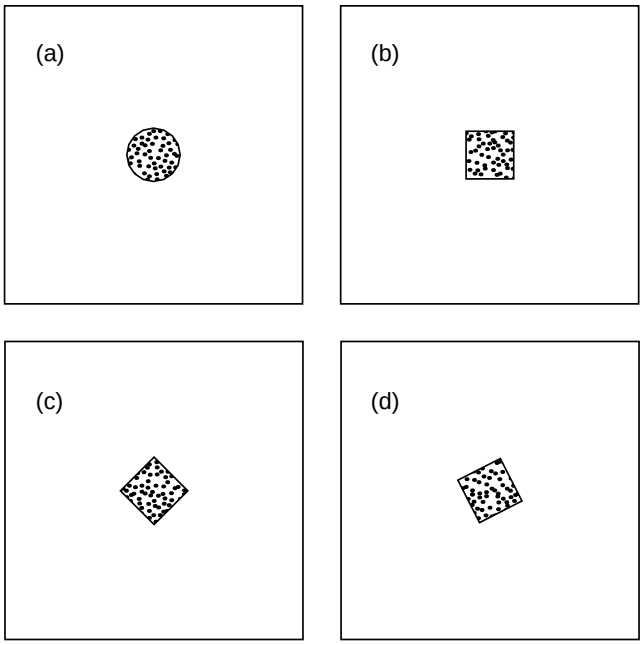

Fig. 1. Two-dimensional models of different shapes of isolated inclusions in a matrix: (a) circle; (b)–(d) squares in three orientations, termed (b) 'square', (c) 'rhomb' and (d) 'skew square' by Treagus and Lan (2000).

The infinitesimal strain of an isolated circular inclusion in a matrix, both with Newtonian viscous properties, a no-slip interface, and in pure shearing, is given by Bilby et al. (1975):

$$\varepsilon_O/\varepsilon_S = 2/\{1 + r\} \tag{13}$$

where ε_O is the inclusion (object) natural strain, ε_S is the bulk or far-field strain, and r is the inclusion-matrix viscosity ratio (μ_O/μ_M). Note that the equivalent expression for a spherical object, given earlier as Eq. (8), is $\varepsilon_O/\varepsilon_S = 5/\{3 + 2r\}$. This difference arises because the third dimension enters into these analyses in different ways (Eshelby, 1957; Freeman, 1987).

2.2. Finite strain of circular and elliptical inclusions

An expression is given by Bilby et al. (1975) for the finite strain of an initially circular inclusion in a matrix, with the same properties as given above. Expressed in terms of the axial ratio (strain ratio) of the inclusion (R_O), the bulk strain ratio (R_S), and viscosity ratio (r) of inclusion to matrix, this

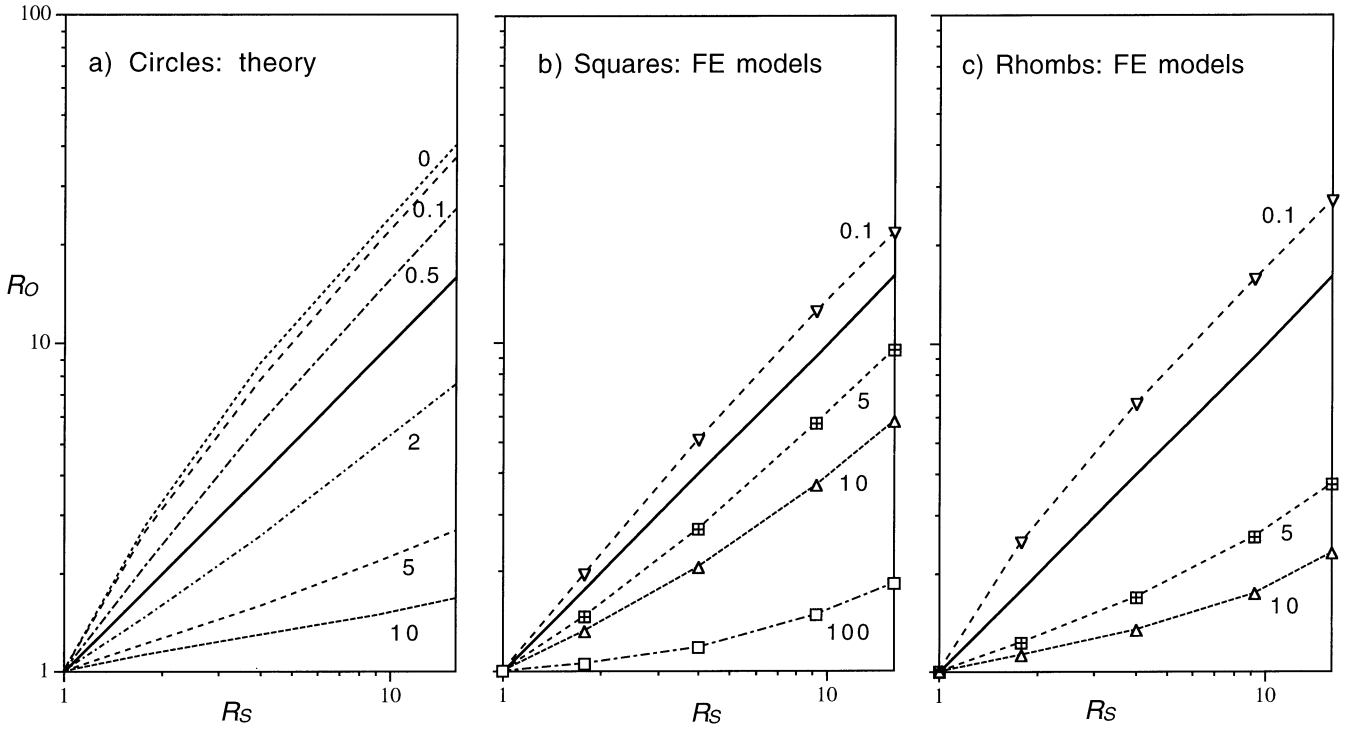

Fig. 2. Graphs of inclusion versus bulk strain on log scales. R_O is the strain ratio of the inclusion or modelled object, and R_S is the bulk strain ratio. Numbers on the broken curves indicate different inclusion/matrix viscosity ratios (r), and the solid diagonal line represents $r = 1$. (a) An isolated circular inclusion in a matrix (Fig. 1a), expressing Eq. (14), (b) 'square' (see Fig. 1b), and (c) 'rhomb' (Fig. 1c) objects, after finite element models (Treagus and Lan, 2000), with the symbols indicating measurements for specific FE models.

is:

$$\ln R_S = \ln R_O + \{(r-1)(R_O-1)/(R_O+1)\} \quad (14)$$

Fig. 2a represents this equation graphically, for a range of r values and up to $R_S = 16$. The curves are slightly non-linear on ln$R$ axes, especially for $r < 1$, and would become more noticeably non-linear if graphed to higher strain values. Treagus and Treagus (2001) have examined the importance of this non-linearity, and its relationship to the growing inclusion ellipticity. They derived an instantaneous inclusion-matrix strain relationship, by differentiation of Eq. (14) with respect to (lnR_O), which can be expressed:

$$\mathrm{d}(\ln R_O)/\mathrm{d}(\ln R_S) = \{(R_O+1)^2/(R_O^2 + 2rR_O + 1)\} \quad (15)$$

This expression has two uses. (i) It describes the infinitesimal strain at any point during the progressive finite deformation of an initially circular inclusion. (ii) It describes the infinitesimal strain for any initially elliptical inclusion aligned parallel to pure shear axes (Treagus and Treagus, 2001). Choosing the latter use, from Eq. (15) the infinitesimal natural strain of an *elliptical inclusion* with axial ratio, R_i, and alignment parallel or perpendicular to pure shearing, is found to be:

$$\varepsilon_O/\varepsilon_S = (R_i+1)^2/(R_i^2 + 2rR_i + 1) \quad (16)$$

This expresses the changing slopes for different r values in Fig. 2a. When $R_i = 1$, which is a circular inclusion, this expression reduces to $\varepsilon_O/\varepsilon_S = 2/\{1+r\}$ as given in Eq. (13).

2.3. Non-elliptical inclusions

Now consider the comparable strain relationships for non-elliptical inclusions, such as the variably oriented *square objects* modelled in finite element (FE) analysis by Treagus et al. (1996) and Treagus and Lan (2000). This latter paper presents a full examination of object versus bulk strain, and the shape development of isolated square objects in three different orientations with respect to pure shear deformation: 'squares', 'rhombs', and 'skew squares' (Fig. 1b–d). These studies demonstrate that isolated non-elliptical inclusions in a contrasting matrix do not generally deform homogeneously. They deform heterogeneously into a variety of shapes, raising the question of how to define an average 'object strain' (R_O). Treagus and Lan (2000) chose to define this strain by the aspect ratios of the transcribing rectangle for 'squares' that deform to irregular barrel, bone, etc. shapes, and the transcribing rhomb for diagonal squares that deform more regularly into near-rhomb shapes. Fig. 2b and c present some of the strain results determined from this FE modelling (Fig. 1b and c).

From comparison with Fig. 2a, it can be seen that if the inclusion is competent ($r > 1$), 'squares' (Fig. 2b) deform significantly more than either 'rhombs' or circles; less if incompetent. The curves are slightly non-linear on ln$R$

axes, but approximately linear over the range of $R_S = 1$ to 4 (= 0 to 50% bulk shortening), suggesting the same relationship for infinitesimal strain as for small to moderate finite strain. The 'rhombs' (Fig. 2c) deformed by almost the same strain as circles with the same viscosity, over this $R_S = 1$ to 4 range. These results and others from Treagus and Lan (2000), together with unpublished finite-element models of other inclusion shapes such as triangles, rectangles and octagons, suggest that the relationships in Fig. 2 for 'squares' and 'rhombs' may bracket the results for an even wider variety of inclusion shapes and strains. Fig. 2b probably represents one extreme: angular inclusions with straight edges subparallel to pure shear axes, such as squares, rectangles and triangles, that deform inhomogeneously into irregular shapes. Fig. 2c represents the other extreme: angular and polygonal inclusions such as diagonal squares, hexagons, and octagons, that strain in almost the same uniform way as circles (Fig. 2a), and whose strains are approximately given by Eq. (14). Between the two extremes will be many inclusions of intermediate behaviour: the skew squares mentioned earlier, and inclusions whose initial shape is intermediate between angular and round (e.g. superellipses; Lisle, 1988; Treagus et al., 1996).

2.4. General expression for $\varepsilon_O/\varepsilon_S$: introducing the shape factor, p

From the preceding sections, the infinitesimal strain of variously shaped inclusions in a matrix in pure shearing can be expressed in the general form:

$$\varepsilon_O/\varepsilon_S = \{(1 + p)/(r + p)\} \quad (17)$$

where $\varepsilon_O/\varepsilon_S$ is the ratio between the inclusion (object) natural strain and the bulk strain, r is the inclusion/matrix viscosity ratio, and p is an additional variable to describe the *inclusion shape factor*. Values of p can be defined for a range of inclusion shapes: theoretically for circular and elliptical inclusions, and empirically from FE model results (Treagus and Lan, 2000). These p values, as listed below, will be used in later modelling of mixtures with different clast shapes (Section 3).

(a) *Circles.* Comparisons of Eq. (13) with Eq. (17) shows that $p = 1$.
(b) *Squares parallel to pure shear axes*. It is found empirically from Fig. 2b that for infinitesimal strain to small finite strain ($R_S < 4$), $p \cong 9$, and thus $\varepsilon_O/\varepsilon_S \cong \{10/(m + 9)\}$.
(c) *Rhombs (squares diagonal to pure shear).* The relationships are found to be approximately those for circles (see Fig. 2c), and so $p \cong 1$.
(d) *Elliptical inclusions with axes parallel to pure shear axes.* Comparison of Eq. (16) with Eq. (17) defines the following relationship:

$$p = (R_i^2 + 1)/2R_i \quad (18)$$

where R_i is the initial or instantaneous ellipse axial ratio (Treagus and Treagus, 2001). From this equation, the p values range from one for a circle, to $p = \infty$ for an infinitely elongate ellipse ($R_i = \infty$), which approximates a strip or layer. In the 'ellipses mixture' modelled in Section 3, $R_i = 5$ and so $p = 2.6$.

Thus, for this range of inclusion-matrix models in pure shearing, the inclusion factor is given as $1 \leq p \leq \infty$. Note that the same p value is found for inclusions of the same ellipticity that are either parallel or perpendicular to the extension direction of pure shear. This is apparent by substituting $1/R_i$ for R_i in Eq. (18).

3. Using two-dimensional inclusion-matrix strain modelling to determine the bulk viscosity of two-phase mixtures

3.1. Mixture geometries and p factors

A single inclusion in a matrix can be considered as a two-phase mixture with a vanishingly small fraction of one phase. Mixtures will now be considered that comprise two viscous phases with measurable fractions, as introduced in Section 1. The material is modelled in two dimensions as a uniform mixture of two phases: phase 1 with area fraction α_1 and viscosity, μ_1, which is the 'weaker' or relatively incompetent phase; and phase 2 with fraction α_2 (where $\alpha_1 + \alpha_2 = 1$) and viscosity μ_2, which is the more competent phase. The phase viscosity contrast, μ_2/μ_1, will be termed m, and according to the above definitions, $m \geq 1$.

Fig. 3 illustrates four idealised mixtures with different grain or clast shapes and p factors, according to definitions in Section 2.4. The first three mixtures have equant clasts of different circular or square shape, and the fourth has aligned elliptical clasts. For illustrative purposes, each mixture is drawn here on a regular (square lattice) pattern, which is not equivalent to an entirely random distribution of phase 2 clasts in a phase 1 matrix. The purpose of this two-dimensional modelling is to investigate the effects of clast shape on the bulk viscosity of a mixture, and so the requirement of statistical isotropy in the self consistent modelling discussed in Section 1.3 for composites of spheres in a matrix, by definition is not met. Instead, the mixtures in Fig. 3 are considered to be a geometrically regular distribution of the two phases that is statistically orthotropic.

The *circles mixture* (Fig. 3a) is illustrated with one circular-grained phase (the competent phase) in a matrix phase, but it can alternatively be a combination of two circular-grained phases (see Section 1.3). As introduced in Section 2.4, this mixture has $p = 1$. Two types of angular-grained mixtures are shown in Fig. 3b and c, both with square clasts, but in different orientations with respect to pure shearing, and so with different effective p values. The diagonal arrangement, termed the *rhombs mixture*, is taken to behave

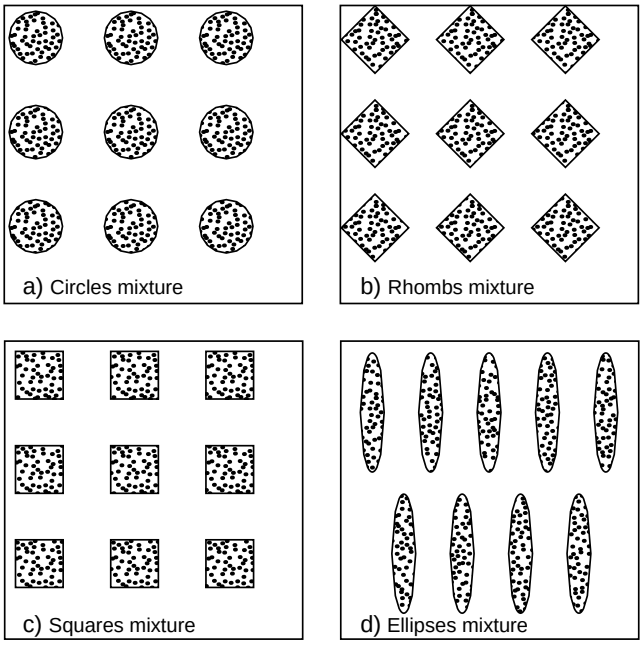

Fig. 3. Idealised two-phase mixtures in two dimensions, comprising one grain or clast phase (shaded; here phase 2), in another particulate or matrix phase (unshaded, phase 1). (a) Circles mixture. (b) Rhombs mixture. (c) Squares mixture. (d) Ellipses mixture, here with clast axial ratio of $R = 5$.

as approximately the same as the circles mixture, with $p \cong 1$. The *squares mixture* with clast edges parallel to axes of pure shearing has $p \cong 9$. The *ellipses mixture* shown in Fig. 3d has clast axial ratios of $R = 5$ and $p \cong 2.6$.

3.2. Determining the bulk viscosity

Following the introduction of the self consistent mechanics (SCM) of composites in Section 1.3, all the mixtures are considered in two dimensions to comprise innumerate inclusions (clasts) of phases 1 and 2, mixed uniformly together. Each clast is assumed to behave and deform as an 'isolated' inclusion in a 'matrix' that has the bulk composite properties. The inclusion-matrix theory and modelling outlined in Section 2 is now employed to define the required functions relating the infinitesimal strain in each fractional phase to the bulk strain. The modelling does not specifically require that clasts are equal-sized, but the SCM method may become increasingly questionable, if there is a large difference among clast sizes.

The inclusion-matrix viscosity ratio, previously denoted $r = \mu_O/\mu_M$, is now expressed for each of the two phases, relative to the bulk viscosity: i.e. as $r_2 = \mu_2/\mu^*$ and $r_1 = \mu_1/\mu^*$. The two-phase viscosity ratio given as $m = \mu_2/\mu_1$ thus equals r_2/r_1. The general $\varepsilon_O/\varepsilon_S$ inclusion-matrix strain relationship for pure shearing (Eq. (17)) will now be written as $\varepsilon_1/\varepsilon^*$ and $\varepsilon_2/\varepsilon^*$ for the two phases, according to their shapes factors (p). (For the SCM method used here, it is necessary to assume the same p values for both phases.) Thus:

$$\varepsilon_1/\varepsilon^* = \{(1 + p)/(r_1 + p)\} \tag{19a}$$

$$\varepsilon_2/\varepsilon^* = \{(1 + p)/(r_2 + p)\} \tag{19b}$$

The SCM method of expressing the bulk strain as the (area) weighted averages of phase strains (Eq. (4)) states:

$$\varepsilon^* = \alpha_1\varepsilon_1 + \alpha_2\varepsilon_2$$

where α_1 and α_2 are the phase area fractions ($\alpha_1 + \alpha_2 = 1$). Substituting Eqs. (19a) and (19b) in this leads to the equation:

$$\frac{\alpha_1}{r_1 + p} + \frac{\alpha_2}{r_2 + p} = \frac{1}{1 + p} \tag{20}$$

Expansion of the r terms into viscosities μ^*, μ_1 and μ_2, and cross-multiplication, produces the following quadratic equation in μ^*:

$$p\mu^{*2} + \{(\mu_1 + \mu_2) - (1 + p)(\alpha_1\mu_1 + \alpha_2\mu_2)\}\mu^* - \mu_1\mu_2 = 0 \tag{21}$$

This is the *general expression for the bulk viscosity* of all the two-dimensional mixtures illustrated in Fig. 3, assuming infinitesimal pure shearing parallel to the axes. It is solvable in μ^* (taking the positive root), if p, μ_1, μ_2 and α_1 or α_2 are known. Note the similarity of this expression to Eq. (10) given for three-dimensional mixtures of spheres in Section 1.3. The expressions are identical if $p = 1.5$ (to be discussed later).

For the *circles mixtures*, we have $p = 1$ and Eq. (21) becomes:

$$\mu^{*2} + \{(\mu_1 + \mu_2) - 2(\alpha_1\mu_1 + \alpha_2\mu_2)\}\mu^* - \mu_1\mu_2 = 0 \tag{22}$$

For an equal-fraction circles mixtures ($\alpha_1 = \alpha_2 = 0.5$), the expression simplifies to:

$$\mu^* = \sqrt{(\mu_1\mu_2)} \tag{23}$$

and so in this case, μ^* is the geometric mean of μ_1 and μ_2.

Consider now various *limiting values* for μ^* given by Eq. (21):

1. Where $\mu_2 = \mu_1$, it is obvious that $\mu^* = \mu_2 = \mu_1$.
2. Where $\alpha_1 = 0$ ($\alpha_2 = 1$), μ^* is equal to μ_2. Where $\alpha_1 = 1$ ($\alpha_2 = 0$), μ^* is equal to μ_1.
3. Where phase 2 approaches rigidity (i.e. $\mu_2/\mu_1 \rightarrow \infty$):

$$\mu^* = \mu_1/\{1 - (1 + p)\alpha_2\} \tag{24}$$

and so the mixture becomes effectively rigid at

$$\alpha_2 = 1/(1 + p) \tag{25}$$

For circle mixtures ($p = 1$), the rigid threshold is at $\alpha_2 = 0.5$. (Recall from Eq. (9) that it was found to be $\alpha_2 = 0.4$ for spheres.) For squares ($p = 9$), it is at $\alpha_2 = 0.1$, which is a very small competent fraction at which effective rigidity is defined.

Table 1
Calculated values of normalised bulk viscosity ($\beta = \mu^*/\mu_1$) for mixtures with four different values (a)–(d) of the two-phase viscosity ratio (m), determined by solution of Eq. (27) at 0.1 increments of phase fractions (α_1, α_2). The three model mixtures have different clast shapes factors (p): circles, $p = 1$; squares, $p = 9$; ellipses with $R = 5$ and $p = 2.6$. The theoretical upper and lower viscous bounds are calculated from Eqs. (1) and (2). These β values are plotted in Fig. 4, and the alternative normalised bulk viscosity (μ^*/μ_2) used in Fig. 5 is given by β/m

$\alpha_1 =$	1.0	0.9	0.8	0.7	0.6	0.5	0.4	0.3	0.2	0.1	0
$\alpha_2 =$	0	0.1	0.2	0.3	0.4	0.5	0.6	0.7	0.8	0.9	1.0
(a) β ($= \mu^*/\mu_1$) values for m ($= \mu_2/\mu_1$) $= 100$ mixtures											
Circles	1	1.24	1.64	2.38	4.17	10.00	23.97	41.98	61.04	80.44	100
Squares	1	2.92	10.68	21.33	32.41	43.61	54.86	66.13	77.41	88.70	100
Ellipses	1	1.52	2.96	8.30	19.36	32.27	45.63	59.14	72.73	86.35	100
Upper bound	1	10.90	20.80	30.70	40.60	50.50	60.40	70.30	80.20	90.10	100
Lower bound	1	1.11	1.25	1.42	1.66	1.98	2.46	3.26	4.81	9.17	100
(b) β values for $m = 10$ mixtures											
Circles	1	1.19	1.46	1.84	2.39	3.16	4.19	5.44	6.86	8.39	10
Squares	1	1.53	2.26	3.12	4.04	5.00	5.98	6.98	7.98	8.99	10
Ellipses	1	1.32	1.79	2.46	3.30	4.28	5.35	6.47	7.63	8.81	10
Upper bound	1	1.90	2.80	3.70	4.60	5.50	6.40	7.30	8.20	9.10	10
Lower bound	1	1.10	1.22	1.37	1.56	1.82	2.17	2.70	3.57	5.26	10
(c) β values for $m = 5$ mixtures											
Circles	1	1.15	1.34	1.57	1.87	2.24	2.67	3.17	3.74	4.35	5
Squares	1	1.29	1.64	2.01	2.41	2.82	3.25	3.68	4.12	4.56	5
Ellipses	1	1.21	1.48	1.80	2.18	2.59	3.03	3.50	3.99	4.49	5
Upper bound	1	1.40	1.80	2.20	2.60	3.00	3.40	3.80	4.20	4.60	5
Lower bound	1	1.09	1.19	1.32	1.47	1.67	1.92	2.27	2.78	3.57	5
(d) β ($= \mu^*/\mu_1$) values for $m = 2$ mixtures											
Circles	1	1.07	1.15	1.23	1.32	1.41	1.52	1.63	1.75	1.87	2
Squares	1	1.09	1.18	1.28	1.38	1.48	1.58	1.68	1.79	1.89	2
Ellipses	1	1.08	1.17	1.26	1.35	1.45	1.56	1.66	1.77	1.89	2
Upper bound	1	1.10	1.20	1.30	1.40	1.50	1.60	1.70	1.80	1.90	2
Lower bound	1	1.05	1.11	1.18	1.25	1.33	1.43	1.54	1.67	1.82	2

4. For the maximum p value ($= \infty$), which describes an infinitely long ellipse or layer:

$$\mu^* = \alpha_1\mu_1 + \alpha_2\mu_2 \tag{26}$$

This is equivalent to the definition of the upper viscous bound, given earlier (Eq. (1)).

5. The equivalent lower viscous bound (Eq. (2)) is only satisfied in Eq. (21) by taking $p = 0$, which is not in the value range of $p = 1 \rightarrow \infty$ for shape fabrics orthogonal to pure shearing.

3.3. Normalised bulk viscosities and numerical results

For purposes of discussion and comparison, it is useful to present the bulk mixture viscosities as dimensionless normalised values. The expression for μ^* (Eq. (21)) can be written as bulk viscosity normalised with respect either to μ_1 or μ_2. Normalisation with respect to μ_1 (the less viscous 'incompetent' phase) is more usual in the rheology and suspensions literature reviewed in Section 1.3 (e.g. Eq. (12)), and is commonly graphed on a log scale. This is the favoured measure in the present study, because it is useful in applications to rocks such as conglomerates, where the matrix is more likely to be the relatively incompetent phase. Normalisation with respect to μ_2 (the more viscous 'competent' phase) appears more commonly in studies of two-phase mineral composites (Section 1.4), usually represented on a linear scale. Results will therefore also be presented in this form, for comparison.

The bulk viscosity normalised to the incompetent phase will here be abbreviated to β ($= \mu^*/\mu_1$). Using $m = \mu_2/\mu_1$ for the two-phase viscosity ratio, and writing in terms of the stiffer fraction (2), Eq. (21) can be written as a quadratic equation in β:

$$p\beta^2 + \{(m - p) - \alpha_2(m - 1)(1 + p)\}\beta - m = 0 \tag{27}$$

Solutions for β ($= \mu^*/\mu_1$) have been calculated for the three mixture models, using their appropriate p values, *circles* (+*rhombs*), *squares* and *ellipses*. The results are calculated in Table 1 and graphed in Fig. 4, for 0.1 increments of phase fraction (α_2) and four values of two-phase viscosity contrasts ($m = 100$, 10, 5 and 2). The alternative normalised viscosities (μ^*/μ_2) are graphed in Fig. 5.

The four specific m values were chosen to simulate a wide range of material mixtures. Models with $m = 100$ approximate to an almost rigid phase in a viscous medium. Values of $m = 100$ and $m = 10$ are the phase contrasts used in Bons's (1993) modelling. Values of $m = 5$ and $m = 2$

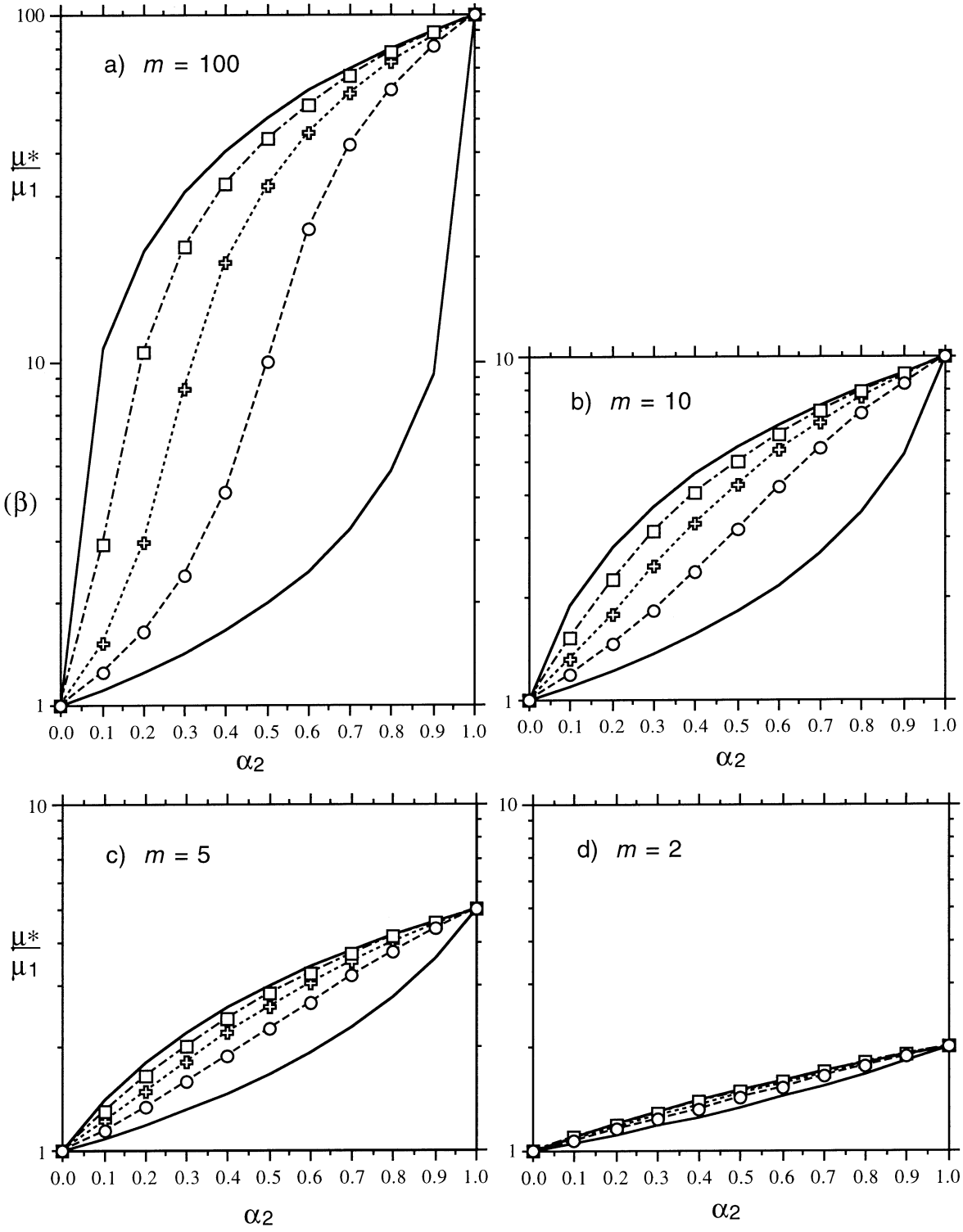

Fig. 4. Bulk viscosities of different mixtures normalised to the incompetent phase ($\beta = \mu^*/\mu_1$), as Table 1, graphed on a log β scale in 0.1 increments of the 'competent' fraction (α_2), for four different two-phase viscosity ratios ($m = \mu_2/\mu_1$): (a) $m = 100$; (b) $m = 10$; (c) $m = 5$; (d) $m = 2$. Circle symbols indicate circles mixtures and (approximately) rhombs mixtures (Fig. 3a and b); square symbols indicate squares mixtures (Fig. 3c); and crosses represent an ellipses mixtures with clast axial ratio, $R = 5$ (Fig. 3d). Solid curves are the upper and lower viscous bounds. See text for full description.

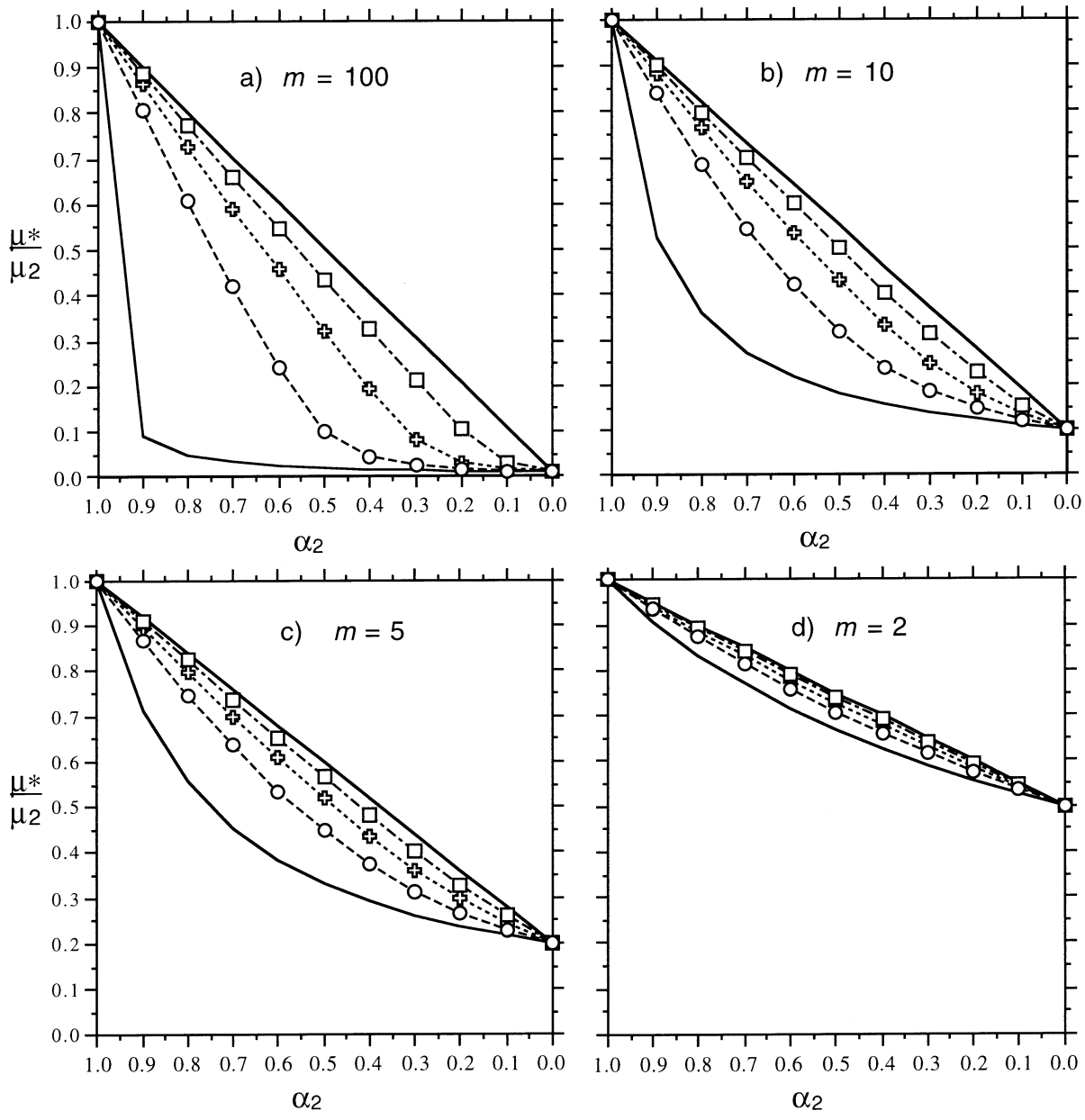

Fig. 5. Bulk viscosities of different mixtures normalised to the competent phase (μ^*/μ_2; see Table 1), graphed on a linear scale in reverse 0.1 increments of the 'competent' fraction (α_2), for four different two-phase viscosity ratios ($m = \mu_2/\mu_1$): (a) $m = 100$; (b) $m = 10$; (c) $m = 5$; (d) $m = 2$. Circle symbols indicate circles/rhombs mixtures, square symbols indicate squares mixtures, crosses represent ellipses mixtures, and solid curves are the upper and lower viscous bounds, as for Fig. 4.

might seem rather small viscosity contrasts, perhaps insufficient to model significant departure from homogeneous behaviour, but such viscosity ratios are suggested among sedimentary rocks in conglomerates and in fold and cleavage-forming processes (Gay, 1968b; Lisle et al., 1983; Treagus, 1999). So together, these m values should encompass the full range of viscous two-phase behaviour.

Fig. 4 graphs values of the normalised bulk viscosity β ($= \mu^*/\mu_1$), on a log scale, for the circles, squares and ellipse mixtures with different two-phase viscosity contrasts (m), in instantaneous pure shear. For each mixture, β increases smoothly with increasing competent phase fraction (α_2). The upper and lower solid lines for each graph are the *upper and lower normalised viscosity bounds*, representing equal strain-rate and equal stress, respectively, in the two phases (Eqs. (1) and (2)). The curves for all three mixtures satisfy the requirement of falling between these bounds. Note how the region between the bounds increases with m, with a wide range of theoretically permissible β values for $m = 100$, but decreasing to near convergence, for $m = 2$. Accordingly, the β values show smaller numerical differences among the different mixtures, for low contrast mixtures. It is apparent that for each different m value (Fig. 4a–d), the three mixtures occupy proportionally

similar positions between the bounds: approximately halfway for circles, and migrating towards positions fractionally nearer to the upper bound with increasing grain shape p factor. (These fractional positions between the bounds will be discussed in more detail in Section 4.2.) No curves are seen to occupy the region between the circles curve, and the lower viscous bound.

Fig. 5a–d shows the bulk viscosities now normalised to phase 2 (i.e. μ^*/μ_2), for the same series of models shown in Fig. 4. These values are graphed on a linear scale with the α_2 scale reversed, to allow easier comparison with the results of Bons (1993), Bons and Cox (1994) and Handy (1994). These graphs have the convenience that all the μ^*/μ_2 values fall in the zero to one range, and now illustrate that the upper viscous bound is linear. Otherwise, the same trends and fractional positions emerge as discussed above for μ^*/μ_1.

Recall that all these results are for mixtures shown in snapshot in Fig. 3: the cross-sectional deformation of 'cylindrical' mixtures, in instantaneous pure shear parallel to the diagram axes. The essential results (Figs. 4 and 5) can be summarised as follows.

(a) *Circles or rhombs mixtures* and isotropic polygonal equivalents ($p = 1$): for all m values, the normalised bulk viscosity curves are positioned approximately midway between the upper and lower viscosity bounds, measured along horisontal lines. This is not a simple mean of the upper- and lower-bound values.
(b) *Squares mixtures* ($p = 9$), where the clasts can deform heterogeneously: the bulk viscosities are greater than those for equal-fraction circles mixtures; i.e. the mixtures are stiffer. Because the normalised values are closer to the upper-bound, this signifies a lesser degree of strain partitioning between the two phases than for circles mixtures.
(c) *Ellipses mixtures*: for $R = 5$ ($p = 2.6$), the bulk viscosity is greater than for an equivalent-area mixture of circles, and it increases progressively with the p factor and grain ellipticity (R), for mixtures with ellipses aligned parallel or perpendicular to pure shearing.
(d) *Bilaminate multilayered mixtures* ($p = \infty$; $R = 0$ or ∞): here, the bulk viscosities are the theoretical maxima, on the upper viscous bound, indicative of homogeneous straining and yielding the stiffest possible mixture.
(e) *Phase viscosity contrasts*: the differences among the normalised viscosity values for the different mixture geometries are progressively smaller, as the two-phase viscosity ratio (m) reduces. At the smallest m value of 2, different mixtures have approximately the same bulk viscosity.

These conclusions all concern the instantaneous response of a mixture with a specific shape fabric, given by p. However, might the results also have some bearing on the changes in bulk viscosity in a deformable two-phase mixture over a progressive pure shear deformation? The progressive deformation would be expected to change the shape fabric of a mixture, and thus alter the p value. For example, the ellipses mixture shown in Fig. 3d would undergo an increase in clast axial ratio (R) during progressive pure shearing in this orientation, and so it might be concluded that the mixture would see a concomitant increase in bulk viscosity over time: i.e. it would progressively stiffen. However, there are difficulties in pursuing these principles, quantitatively, because in the two-dimensional model used here (and implicit in the SCM method), the two phases must have the same p factor. For circular to elliptical fabrics, p is directly related to ellipse axial ratio, R, and in the finite straining of a two-phase mixture, it would be expected that *different* R values would emerge for the two phases: with R_1 (incompetent grain phase) becoming progressively greater that R_2 (competent phase). To model progressive changes, accurately, it would therefore be necessary to adopt progressively different p factors for the two phases, which contravenes the present approach. Qualitatively, however, it can be said that because *all* p factors will increase with progressive deformation, even if at different rates, these clastic two-phase mixtures will become progressively more viscous and stiffen, as pure shearing progresses.

4. Discussion

4.1. Comparisons with previous models of geological mixtures

The preceding results will now be compared with relevant results for geological mixtures, reviewed in Section 1.4. The μ^*/μ_2 curves for $m = 100$ and 10 circles mixtures (Fig. 5a and b) are found to be very close to Bons's results of finite-element modelling of isotropic mixtures (Bons, 1993; fig. 7.17). He used two FE model series: (a) with elastic behaviour and hexagonal elements; (b) using power-law (including stress exponent = 1, equivalent to a viscous model), and square grain elements. His results from the two series are indistinguishable, with the phase contrasts of 10 and 100. It should be noted that Bons's square 'grains' are not directly comparable with my squares mixture that is based on FE models of the single square inclusions by Treagus and Lan (2000). In this, the inclusion is a square made up 64 smaller square elements, so allowing the possibility of strongly heterogeneous deformation (e.g. to barrel shapes). Bons's square 'grains' in his (b) series comprised only two triangular elements, which in practice will amount to homogeneous grain deformation, so are more comparable with the circular inclusion. This may explain the similarity of results from Bons's two different models, despite their different 'grain' shapes: both immeasurably close to my circles mixtures for $m = 100$ and 10 (Fig. 5a and b). Bons's 'horizontal distance' factor will be discussed in the next section.

It is more difficult to make direct comparisons of these

results with models derived for non-linear rocks or analogues, or with laboratory results that are derived from uniaxial deformation. Nevertheless, Jordan's (1987, fig. 4G) bulk strength curve for limestone–halite mixtures is broadly similar to the μ^*/μ_2 curve for circles mixtures ($m = 10$; Fig. 5b). The $m = 5$ mixtures shown in Fig. 5c are found to be qualitatively similar to the FE model simulations of pyroxene–plagioclase aggregates by Tullis et al. (1991, fig. 9a), for their 10^{-12} s^{-1} strain rate series, which has an effective phase strength contrast of $\cong 4.2$ according to their fig. 6(a). Most of the models of Tullis et al. (1991) have square elements, but two data points are provided for circular grain elements. Despite the assumption of my modelling of Newtonian viscous behaviour, and theirs using non-linear flow laws to model plagioclase and pyroxene, the results are similar. Their models appear to confirm that mixtures of square grains with edges parallel to pure shear (so long as the 'grains' are allowed to deform heterogeneously) will behave more stiffly, and closer to the upper bound, than mixtures of round grains. It follows that the strain will be partitioned less in these types of angular mixtures (also observed by Bloomfield and Covey-Crump (1993)), than in equivalent round-grained mixtures.

The normalised viscosity curves shown in Fig. 5 for my models of mixtures are found to be distinctly different from those deduced by Handy (1994, fig. 9) for $m = 10$, 5 and 2. However, it was noted earlier that Handy's results are for simple shear, and they also depend on an unverified function for strain rate partitioning in the incompetent fractions, that may be appropriate to strain partitioning among layers rather than grains. Handy's curves appear to be qualitatively close to the theoretical lower-bound values for the chosen phase contrasts. Further comments on the interplay among bulk viscosity and mixture geometry, and comparisons of pure and simple shear deformation, will be given in Section 4.3.

4.2. Constant relative horizontal distance, H

An important conclusion of Bons (1993) and Bons and Cox (1994) was that for their mixtures with a certain geometry (modelled by strings of grain 'elements'), the bulk viscosity value was at a constant horizontal fractional distance (termed *H*), in the space between the upper and lower viscosity (or strength) bounds. This result is also suggested by the curves shown here in Figs. 4 and 5, and will now be assessed more accurately. However, first an important difference needs to be noted between the results in Bons and Cox (1994, fig. 2) for normalised elastic stiffness of anisotropic mixtures, and those for normalised viscosity shown in Fig. 5. In both methods, an anisotropy factor appears to control the positions of curves. In my method, this is the *p* factor, which importantly has the same value for ellipses mixtures, whether the 'grains' are parallel or perpendicular to the pure shear extension. (Oblique orientations are not modelled.) In contrast, the models of Bons and Cox (1994, fig. 2) showed a different fractional distance (*H*), for anisotropy given by 'strings' of four or eight grain elements that were parallel to extension, compared with those that were perpendicular. The difference between their results and mine appears to lie in different definitions of bulk behaviour. Bons and Cox define 'composite stiffness' as the average normal stress in the direction of extension. Where there is anisotropy, this measure of stiffness is not directly equivalent (by elastic-viscous correspondence principles) to the bulk viscosity of viscous mixtures determined by my method. According to their method, layered systems parallel and perpendicular to pure shear extension would not behave the same; i.e. *not* both falling on the upper bound, as in my model. For this reason, direct numerical comparisons will not be made between the two approaches, for anisotropic mixtures.

Although Bons and Cox do not prove that *H* is constant for any of their models, their model results are shown to fall close to graph curves of constant *H* (e.g. Bons and Cox, 1994, fig. 2). It was noted earlier that all the circles mixtures in Figs. 4 and 5 occupy approximately half-way horizontal positions between the bounds. It can now be examined whether the mathematics confirms *H* to be *exactly* 0.5, and whether a constant *H* value can be defined in terms of all particular *p* values. Fig. 6 illustrates the definition of 'relative horizontal distance', *H*, after Bons (1993) and Bons and Cox (1994), where *H* is the fraction *a/d* along any horizontal. Writing in terms of measures of the weak fraction (α_1), between the lower (Reuss) strength/viscosity bound (subscripted L), and the upper (Voigt) bound (subscripted U), measured from low to high, and using

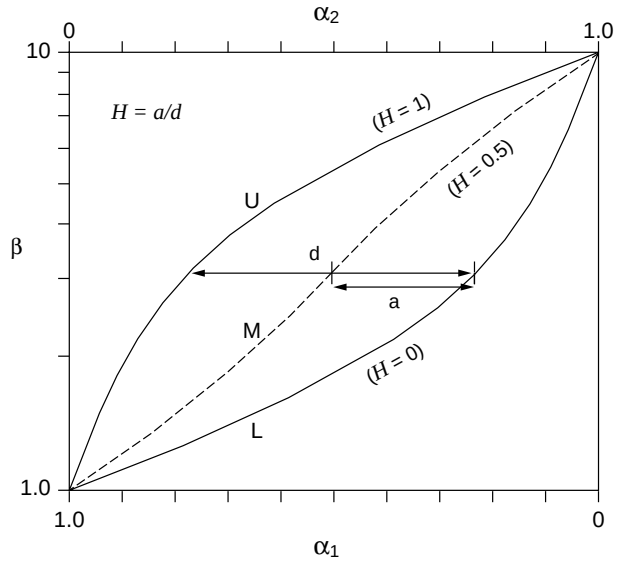

Fig. 6. Definition of 'relative horizontal distance', *H*, of Bons (1993) and Bons and Cox (1994). The example is after Fig. 4b, with U and L curves showing the upper and lower viscous bounds, respectively, and M representing a mixture (here, the circles mixture). Their respective *H* values are shown.

subscript M for the mixture curve:

$$a = (\alpha_{1(M)} - \alpha_{1(L)}), \text{ and } d = (\alpha_{1(U)} - \alpha_{1(L)}) \quad (28)$$

Thus:

$$H = (\alpha_{1(M)} - \alpha_{1(L)})/(\alpha_{1(U)} - \alpha_{1(L)}) \quad (29)$$

Now write all the α_1 terms as functions of the normalised viscosity, β ($= \mu^*/\mu_1$).

For the mixture, rearrangement of Eq. (27) determines $\alpha_{1(M)}$ to be:

$$\alpha_{1(M)} = \{(m - \beta)(1 + p\beta)\}/\{(1 + p)(m - 1)\beta\} \quad (30)$$

For the upper bound, from Eq. (1):

$$\alpha_{1(U)} = \{(m - \beta)/(m - 1)\} \quad (31)$$

For the lower bound, from Eq. (2):

$$\alpha_{1(L)} = \{(m - \beta)/(m - 1)\beta\} \quad (32)$$

Substituting these terms in Eq. (29), m and β are found to cancel out to produce the following expression for H as a simple function of p:

$$H = p/(1 + p) \quad (33)$$

Thus the constant 'relative horisontal distance' of Bons is proved.

For *circles mixtures*, $p = 1$ in Eq. (33) clearly gives $H = 0.5$, which provides accuracy to the earlier observations of 'approximately half'. For *squares mixtures*, $p = 9$ gives $H = 0.9$, and the example of *ellipses mixtures* with $p = 2.6$, gives $H = 0.72$, as shown in Figs. 4 and 5. Other ellipse axial ratios (R) will have different H values. Recalling from Eq. (18) that

$$p = (R^2 + 1)/2R$$

this leads to the direct relationship of H and ellipse axial ratio, R:

$$H = \{(R^2 + 1)/(R + 1)^2\} \quad (34)$$

By definition, the *upper bound* has $H = 1$, verifying that here, $R = 0$ or ∞, with $p = \infty$ (i.e. layers). The *lower bound* has $H = 0$, with no real solution for R, again showing that no solutions can fall on the lower bound or have $p = 0$, when the shape fabric is orthogonal to pure shearing.

This horizontal distance measurement, H, is a potentially useful tool for defining the bulk viscous properties of mixtures, and for extrapolating to other mixtures. All the mixtures with shape fabrics parallel or perpendicular to pure shear had normalised bulk viscosities occupying the 'upper halves' of the region between the upper and lower bounds, in Figs. 4 and 5: i.e. with $0.5 \leq H \leq 1.0$ (see also Fig. 7). The next section will consider the meaning of the 'lower half', and whether any two-dimensional two-phase mixtures have bulk properties with $H < 0.5$.

4.3. Extrapolations for mixtures with orthogonal or diagonal shape fabrics: pure shear, simple shear and anisotropy

The results of the two-dimensional modelling are now discussed in a broader context, by considering the effects of the shape fabric and orientation with respect to instantaneous deformation on normalised bulk viscosities. A two-phase system with moderate viscosity contrast of $m = 10$ will be used for illustration, beginning with the β values of normalised viscosity (μ^*/μ_1) shown in Fig. 4b for pure shearing of orthogonal circle/ellipse mixtures. These are first extrapolated to mixtures with diagonal fabrics in pure shearing, and then to simple shearing orthogonal or diagonal to the shape fabrics. The results are compiled in Fig. 7, using the preferred β log-scale graph, because the rotational symmetry aids the extrapolations.

As noted previously, β values for mixtures with *orthogonal shape fabrics in pure shearing* with $1 \leq p \leq \infty$ all occupy the 'upper half' of the permissible field between the upper and lower viscous bounds (i.e. $0.5 \leq H \leq 1$). This region is shown in Fig. 7 by the orthogonal hatching, and mixtures with increasing elliptical clast fabrics (given by numbered axial ratios, R) occupy positions progressively closer to the upper viscous bound. The half-way curve ($H = 0.5$; $p = 1$; $R = 1$) can be considered to represent statistically isotropic mixtures in two dimensions, such as those with circular-grained fabrics. The upper bound ($H = 1$) represents the bulk viscosity in cross-sections of a bilaminate multilayer in pure shear parallel or perpendicular to layering ($p = \infty$, 'ellipses' with $R = \infty$). Recall from Section 1.2 and Eq. (1) that the equation for the upper bound has identical form to that for the normal viscosity (μ_n) for a layered (statistically anisotropic) medium (Biot, 1965, pp. 186 and 432; Cobbold, 1976). The whole 'upper half' of Fig. 7 records the interrelationships of shape fabric, material anisotropy and bulk viscosity. The bulk viscosity determined for these mixtures with their shape fabrics aligned parallel/perpendicular to pure shearing, is strictly measuring the *bulk normal viscosity* (μ_n^*) (the relationship of normal stress and normal strain rate) parallel or perpendicular to the shape fabric of the anisotropic mixtures. Thus, the hatched region is the normalised normal viscosity, β_n.

Fig. 4 revealed no solutions for β in the 'lower half' of the permissible bulk viscosity field ($H < 0.5$). Such a solution to Eq. (27) would require $0 \leq p \leq 1$. However, it was noted in Section 1.2 that Eq. (2) for the lower viscous bound has an identical form to that for the shear viscosity (μ_s) for a layered anisotropic medium (Biot, 1965, pp. 186 and 432; Cobbold, 1976). The lower bound in Fig. 7 can thus be considered to have two physical meanings, in terms of the bulk viscosity of layered mixtures or bilaminates. (a) It represents the shear viscosity, μ_s (the relationship of shear stress and shear strain-rate) parallel to layering, in normalised form (β_s). (b) Alternatively, it represents the normalised normal viscosity (β_n) at 45° to layering.

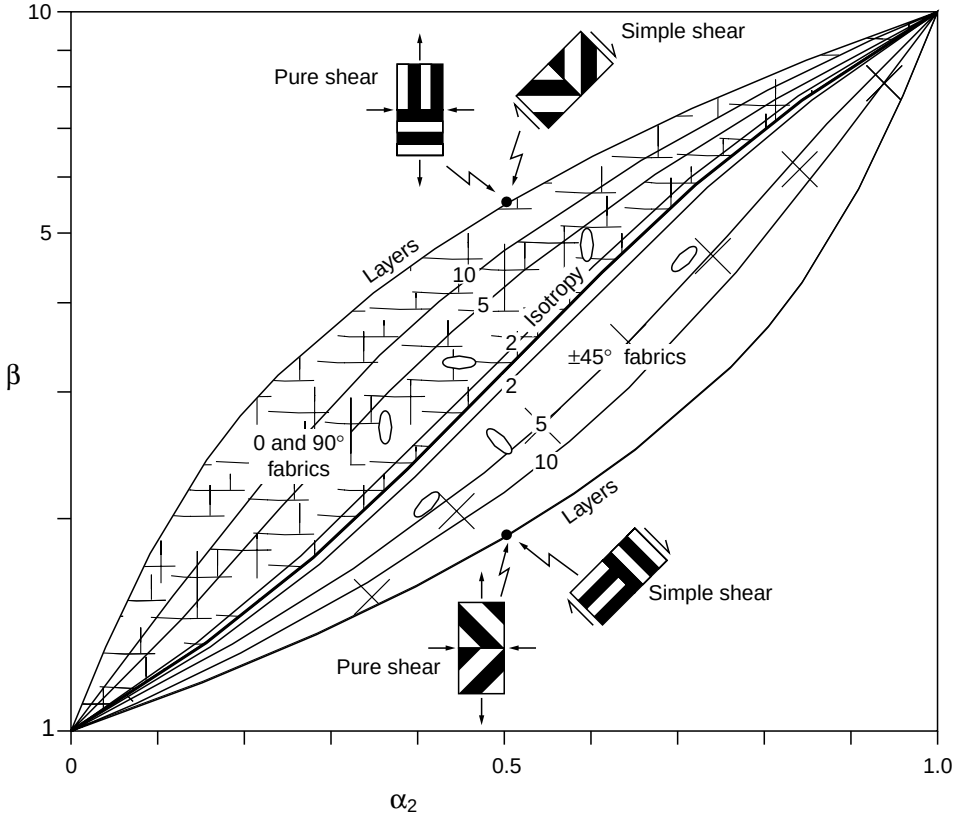

Fig. 7. Extrapolations leading to generalised relationships of the normalised bulk viscosity ($\beta = \mu^*/\mu_1$) of two-phase mixtures, according to the degree of two-dimensional shape fabric and its orientation relative to instantaneous deformation. This example has a two-phase viscosity ratio of $m = 10$, after Fig. 4b. The upper and lower bounding curves indicate the bulk viscosity for end-member layered mixtures (see insets). The hatched symbols in the 'upper half' of the graph show mixtures with progressively elliptical shape fabrics (axial ratio, R, numbered on curves) in the orientation shown, orthogonal to pure shearing (or in simple shearing at ±45°). The diagonal cross symbols in the 'lower half' of the graph indicate the bulk viscosity for the mixtures with the same elliptical shape fabrics (given by numbered R values), but oriented diagonally in pure shearing (or parallel/perpendicular to simple shearing). Note the 180° rotational symmetry of the curves for each Rvalue in the two 'halves'. The ordinate distance between like-numbered curves is the value of the bulk viscous anisotropy: see text for further discussion.

An interesting relationship is apparent, when the normalised viscosities are graphed on a log-scale (e.g. Figs. 4 and 7): the curves for the upper and lower bounds have 180° rotational symmetry. The 'central' $p = 1$ ($H = 0.5$) curve for isotropic 'circles' mixtures is also rotationally symmetric. Thus, it is possible to transpose *all* the R curves in the upper half of Fig. 7 (for pure shearing of orthogonal fabrics), through rotation, to occupy the vacant lower half of the graph. These can now be considered to represent the curves for mixtures with the same shape-fabrics, but oriented at 45° to pure shearing. The 'lower half' of Fig. 7 fills exactly the same space and shape as the 'upper half', with the same limits: isotropic (circle) fabrics on the middle edge, and layered fabrics on the outer edge. All the calculated R curves for the orthogonal fabrics in pure shearing, when transposed by rotation to lower half (diagonal crosses, Fig. 7), represent curves for the normalised viscosity (β) of mixtures with *diagonal shape fabrics in pure shearing.*

The above extrapolations are restricted only to mixtures of circles to ellipses (to the limit of layers): clast shapes that according to the inclusion-matrix theory undergo homogeneous strain. In non-elliptical inclusions such as squares, the finite element modelling (Treagus and Lan, 2000) that underpins these angular-grained model mixtures showed that the orientation affects their degree of heterogeneous strain. Thus, although the rhombs mixture is geometrically a diagonal form of the squares mixture, the symmetry arguments applied to ellipses and layers in parallel and diagonal orientations, used in Fig. 7, cannot so simply be applied to angular-grained mixtures. For this reason, this part of the discussion of mixture rheology and shape fabric focuses only on shape fabrics in the circle/ellipse/layer spectrum.

What is the relationship between the p and H factors calculated for the orthogonal mixtures in the upper half of Fig. 7, and those extrapolated for diagonal fabrics with the same R value, in the lower half? Writing primed values for the diagonal fabrics, it is apparent from Fig. 7 and Eq. (33) that:

$$H' = 1 - H;\ p' = 1/p \tag{35}$$

This confirms that the p range for orthogonal fabrics in

pure shearing, of $1 \leq p \leq \infty$, converts into the range of $1 \geq p' \geq 0$ for diagonal fabrics in pure shearing with the same R values ($1 \leq R \leq \infty$).

The results and extrapolations in the upper and lower fields of Fig. 7 also represent the *anisotropy of bulk viscosity* of these mixtures relative to a particular direction. The hatched upper region represents normalised normal viscosities ($\beta_n = \mu_n^*/\mu_1$), and those in the crossed lower region represent normalised shear viscosities ($\beta_s = \mu_s^*/\mu_1$), measured parallel or perpendicular to the shape fabric. The ratio of these two normalised values (β_n/β_s) thus provides a direct measure of the bulk anisotropy (μ_n^*/μ_s^*): this can be measured in Fig. 7 as the *linear* ordinate-parallel distance between like-numbered curves. In this example with a two-phase viscosity ratio of $m = 10$ (Fig. 7), for an equal-fraction mixture ($\alpha_1 = \alpha_2 = 0.5$), the anisotropy of a bilaminate mixture is $\cong 3$, and for an $R = 5$ ellipses mixtures, it is $\cong 1.7$. These mixtures are stiffer in normal stress than shear stress. The same principles also apply to anisotropy measured diagonal to shape fabrics, but the values of μ_n^* and μ_s^* will be now exchanged, so that $\mu_s^* > \mu_n^*$, and so these mixtures are stiffer in shear than in normal stress.

Fig. 7 cannot directly represent the normalised bulk viscosity of mixtures with fabrics in oblique orientations, between orthogonal and diagonal with respect to pure shearing. A mixture of aligned elliptical clasts with $R = 5$ would be expected to have bulk properties falling proportionally between those in the upper and lower fields for orthogonal and diagonal fabrics, respectively, according to the fabric orientation, but the exact position cannot be determined from this diagram.

Consider now *simple shearing* of these models of circular/elliptical/layered mixtures. For instantaneous plane-strain deformation, a simple shear parallel to x can be considered equivalent to pure shear oriented at 45° to x, plus a small rigid rotation (see Hobbs et al., 1976, p. 32). This can also be verified by the solutions for inclusion strain rates relative to bulk strain rates for elliptical inclusions in different orientations, for pure and simple shear (Bilby and Kolbuszewski, 1977, eqs. 28 and 34). So it follows that the results shown for pure shear in Fig. 7 can also be considered to represent the instantaneous response of the same mixture geometries, but in simple shear at ±45° to the graph axes. Now the upper bound represents a bilaminate multilayer in simple shear at 45° to layering; the lower bound represents simple shear parallel or perpendicular to layering (see Fig. 7 insets). All the same extrapolations made above for parallel and diagonal fabrics in pure shear can now be made for simple shear, with the same implications for bulk viscous anisotropy. The hatched upper region thus represents values for shape fabrics progressing from circular (isotropic) through elliptical to layered, in simple shearing diagonal to the fabric (i.e. 45°-diagonal to the graph axes in Fig. 7). The lower half represent mixtures that are in simple shearing parallel or perpendicular to the fabric.

To speculate further, to consider the *progressive behaviour* of these mixtures in either pure or simple shearing, is not straightforward. As discussed at the end of Section 3.3, fabric ellipticities will change with progressive deformation, suggesting progressive changes in H, but the present model does not allow for the development of *different* degrees of elliptical fabric in the two phases. All that might reasonably be concluded, therefore, is that a mixture undergoing pure shear deformation, that increases the ellipticity of the shape fabric parallel to the strain axes, would be expected to have progressively upward-migrating instantaneous β curves in the upper half of Fig. 7, indicating some progressive stiffening.

For diagonal fabrics in pure shear, and for all fabric orientations in simple shear, the progressive changes of bulk viscosity are likely to be more complicated, because these deformations will also rotate the shape fabric. At the extreme, certain types of shape fabrics in long-lived steady simple shearing might undergo cycles of straining and unstraining (and associated changes in phase R values), that would mean that the bulk properties also cycled between relative stiffening and relative softening over time. Such processes, if they operate, have analogies with the theoretical cyclic or oscillatory flow histories described for single inclusions in simple shear (Bilby and Kolbuszewski, 1977) or in fluid flow (Ghosh and Ramberg, 1976; McKenzie, 1979).

This part of the discussion has largely focused on the example with a phase contrast of $m = 10$ (Fig. 7). It is clear from Figs. 4 and 5 that the value ranges of the normalised viscosities (enclosed by the upper and lower viscous bounds) are strongly dependent on the chosen m values of these theoretical mixtures, and this will also affect extrapolations such as perceived viscosity changes over a progressive deformation. For weakly contrasting two-phase mixtures (e.g. $m = 2$), where the upper and lower bounds are quite close together, the bulk properties will not differ greatly among mixtures with different shape fabrics, the material will not be markedly anisotropic, and it is therefore unlikely that the bulk viscosity will change very much during a progressive deformation. The material properties might be considered approximately constant over time and space. At the other extreme, a high phase viscosity contrast (e.g. $m = 100$) might be expected to behave approximately as a rigid phase in a viscous phase, with a wide range of possible bulk viscosity bounded by the upper and lower limits, and governed by the shape fabric of the competent phase, which also determines the degree of viscous anisotropy, as recently modelled by Mandal et al. (2000). However, as the clast shape of this pseudo-rigid phase will not change perceptively over a progressive deformation, the bulk viscosity may also remain approximately constant over time. It is therefore only at moderate values of two-phase viscosity ratios, such as $m = 5$ or 10, that the bulk viscous properties of two-phase mixtures are likely to change significantly over progressive deformation.

However, these are the kinds of viscosity contrasts indicated from studies of deformed conglomerates and other structures (Gay, 1968b; Lisle et al., 1983; Treagus, 1999).

4.4. Three-dimensional modelling

All the results discussed above concern two-dimensional modelling of mixtures of different types. In three dimensions, these must be considered as 'cylindrical' mixtures, as illustrated for the 'circles mixture' in Fig. 8a. Such mixtures might be considered as viscous analogies to fibre composites: materials that are transversely isotropic, with elastic properties of considerable interest in materials science and applied mechanics (Hashin, 1983). The two-dimensional model results given in Table 1 and Figs. 4 and 5 for normalised bulk viscosities of mixtures (circles, squares, ellipses, layers) may thus provide a method of determining the 'transverse' properties of cylindrical or fibrous mixtures (Fig. 8a, face A). The 'longitudinal' properties would refer to faces B or C in Fig. 8a, where according to this modelling, all the mixtures would appear to be 'layered', and thus the bulk viscosity would follow the upper bound curves given by Eq. (1). These differences, of course, reveal the three-dimensional anisotropy (Mandal et al., 2000) of 'cylinder' mixtures.

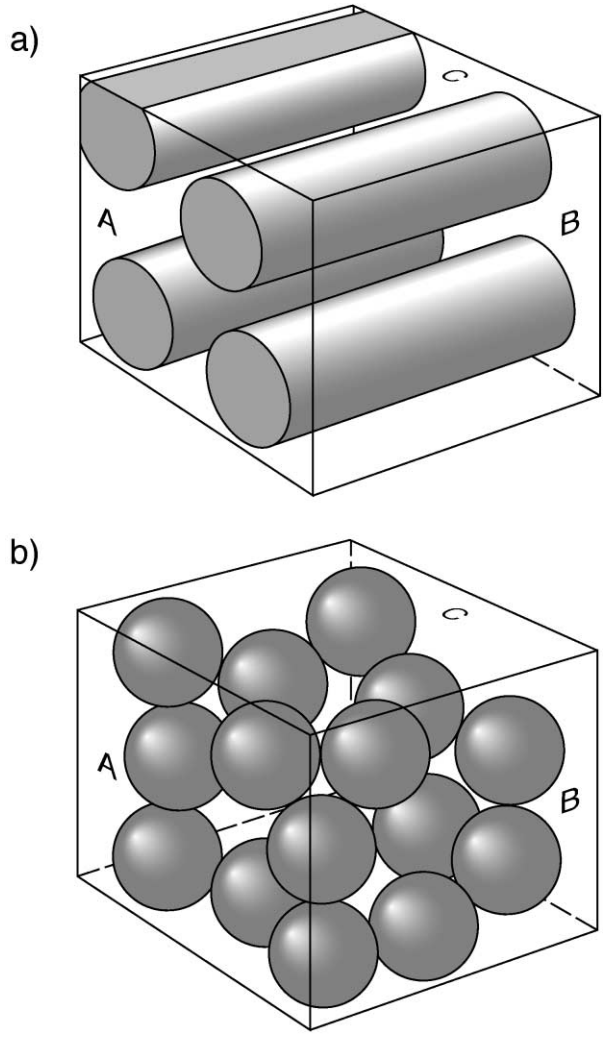

Fig. 8. Comparisons of round-grained mixtures in two and three dimensions. (a) Two-dimensional *circles mixtures* are 'cylindrical' in three dimensions. (b) Randomly isotropic *spheres mixtures*, as envisaged for suspensions and for analysis of composites by self consistent mechanics (SCM). Faces A, B and C in each are referred to in the text.

A more appropriate three-dimensional version of the circles mixture for rocks might be a mixture of spheres, as depicted in Fig. 8b. This is the model discussed in the Introduction (Section 1.3), in connection with statistically isotropic composites and self-consistent mechanics (SCM). The bulk viscosity determined by the SCM method for plane-strain pure shear was given by Eq. (10). The same bulk viscosity would be determined for all three principal sections of pure shearing (Fig. 8b; faces A, B and C), and is not equal to the result determined in the two-dimensional analysis (face A in Fig. 8a): i.e. Eq. (10) is not equivalent to Eq. (22). The differences arise from the use of different expressions for inclusion-matrix strain (after Eshelby, 1957; Bilby et al., 1975) for spheres and cylinders in pure shear, and are illustrated in Fig. 9a for two examples of phase contrast ($m = 10$ and 100). They can be quantified by different values of H (relative horizontal distance; Fig. 6): $H = 0.5$ for the two-dimensional circles mixture, and $H = 0.6$ for spheres (comparable with an ellipses mixture with $p = 1.5$ and $R = 2.6$). It is paradoxical that a truly isotropic mixture of spheres does *not* occupy the 'half way' positions ($H = 0.5$) between the upper and lower bounds, in the same way that the isotropic circles mixtures does in two dimensions.

It must be asked whether the two-dimensional results produced in this paper, showing simple and direct relationships between clast shape and bulk viscous properties of two-phase mixtures, have any useful applications to real geological mixtures in three dimensions. It is certainly not suggested that rocks are generally mixtures of rods or cylinders, as shown in Fig. 8a. However, beyond perhaps the first instant of deformation, rocks are not mixtures of perfect spheres, either. No explicit solution for the instantaneous deformation of *ellipsoidal inclusions* in a matrix is available (see Freeman, 1987), that would lead via self consistent modelling to expressions for bulk viscosities of two-phase clast mixtures in terms of three-dimensional clast shapes (ellipsoid axial ratios). The choice at present is between results for three-dimensional mixtures restricted to spheres-only; or the limitations of two-dimensional modelling of mixtures with a range of aligned clast shapes, to model a shape fabric. If the two-dimensional models underestimate the bulk viscosity in pure shearing, to some degree, the difference can only be assessed for circles versus spheres (i.e. isotropic mixtures), as shown in Fig. 9a. This is a difference of 10% in H, and is probably the maximum possible difference, reducing progressively with increasing shape fabric, because the two- and three-dimensional methods are both restricted by the same upper and lower

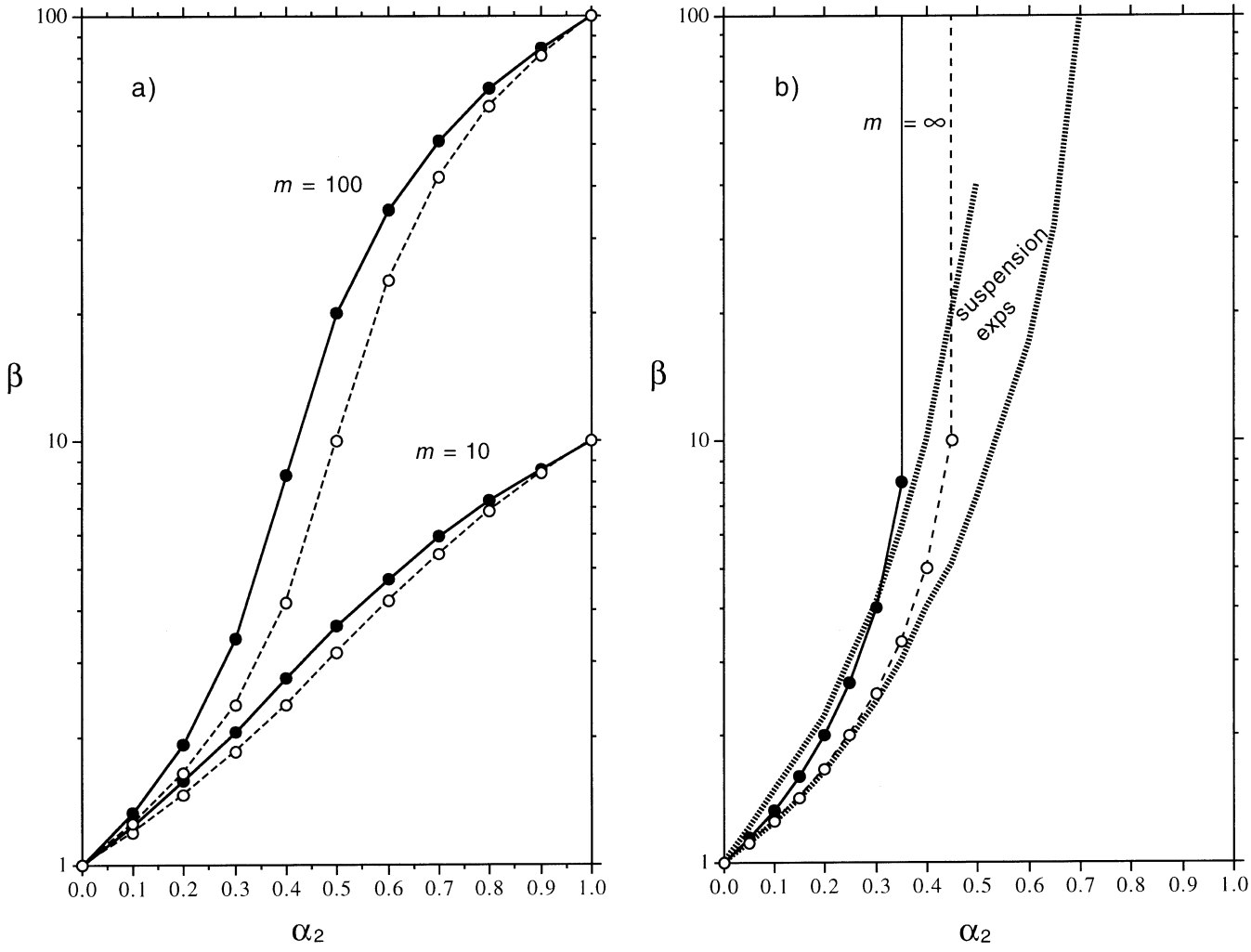

Fig. 9. Comparisons of the values of normalised bulk viscosities ($\beta = \mu^*/\mu_1$) determined from two- and three-dimensional analyses of 'isotropic' two-phase composites: solid circles and solid curves indicate three-dimensional *spheres mixtures* (Eq. (9)); open circles and broken curves are the two-dimensional circles mixtures of this paper (Eq. (27); Table 1). (a) Results for m ($= \mu_2/\mu_1$) = 100 and 10. The two curves have different H values (Fig. 6): $H = 0.6$ for spheres, and $H = 0.5$ for circles. (b) Theoretical curves for spheres and circles mixtures as in (a), but taking $m = \infty$. The two superimposed shaded curves bracket the region given by a number of series of experiments with suspensions of rigid spheres in a fluid (after Collyer and Clegg, 1988, fig. 16.14; Ferguson and Kemblowski, 1991, fig. 6.16).

bounds. For this reason, it does not seem unreasonable to use the results given in Figs. 4 and 5 as an approximate trend for sectional behaviour of truly three-dimensional spherical/ellipsoidal mixtures, even if underestimating the H-values of the curves by up to 10%.

The most important finding for rocks from the preceding two-dimensional modelling is that elliptical fabrics make stiffer mixtures in pure shear than circular mixtures with the same phase fractions. So it might reasonably be concluded that *ellipsoidal fabrics* in principal sections of pure shearing will likewise have bulk viscosity that increases with sectional ellipticity. Such a mixture would be anisotropic, but in a different manner from the cylindrical mixture shown in Fig. 8a. In terms of strain (or shape fabric) ellipsoid axes, the bulk viscous properties and anisotropy would mirror these shape fabric values and directions, as considered for rigid clasts in a matrix by Mandal et al. (2000).

It was suggested, earlier, that mixtures of two phases with $m = 100$ might approximately model a rigid phase in a viscous phase. However, with a truly rigid phase, m approaches infinity, and the mixture properties reduce to the relationships given in Eq. (11) for spheres, and Eq. (25) for circles, ellipses, etc. As discussed above, this particular end-member case of a 'solid' phase in a 'liquid' phase has been widely analysed, theoretically (see Collyer and Clegg, 1988, pp. 487–493 and 625–632), and provides experimental data with which to compare the modelling presented in this paper. Fig. 9b presents a compilation of experimental modelling of the normalised viscosity, β (known in applied rheology terminology as 'relative viscosity'), for suspensions of spheres in a viscous fluid,

after Ferguson and Kemblowski (1991, fig. 6.16) and Collyer and Clegg (1988, fig. 16.14). The 'spheres' and 'circles' curves for $m = \infty$ are superimposed, showing β approaching infinity at $\alpha_2 = 0.4$ and 0.5, respectively, as discussed earlier. Neither curve forms a central fit for all the experimental data. The spheres curve is closer for low α_2 fractions (<0.2), whereas the circles curve matches the data better for $\alpha_2 = 0.3$–0.45. Interestingly, the pair of $m = 100$ curves in Fig. 9a provide equally good fits to the experiments, for low fractions, to those shown for $m = \infty$, and fill the experimental range somewhat better for medium to high fractions. So if seeking a purely empirical relationship, the $m = 100$ curves for either spheres and circles could be used to approximate the bulk viscosity for a mixture of a rigid phase in a fluid phase, within limits.

It is concluded that two-dimensional modelling and derivation of Eqs. (21) and (27), relating the bulk viscosity of two-phase mixtures to clast shapes, may provide a valid approximation to the bulk viscous properties of mixtures in three dimensions. Recall from the Introduction that many of the established methods of quantifying the bulk properties of composites are also approximations, based on variational bounds or statistical averaging and principles of self-consistent mechanics. Accordingly, all are open to critical discussion for ignoring processes such as the mutual interactions of the phases, which might legitimately limit the analysis to low concentrations of one phase in another (e.g. $\alpha_2 < 0.2$), or the effects of scale (mixtures of small and large clasts), or processes such as microstructural changes. With these uncertainties in mind, the simple two-dimensional analysis provided here, and the results given in Figs. 4 and 5, can provide some useful rules and approximations for the behaviour of two-phase mixtures with initial or progressive shape fabrics, of potential application to a variety of rocks from conglomerates to crystalline aggregates.

5. Conclusions

Many types of rocks, including conglomerates, can be considered as multiphase mixtures. At their simplest, these can be modelled as two-phase mixtures. This paper provides two-dimensional modelling of a variety of mixtures of clasts idealised as circles, squares or ellipses. Added to these are end-member cases of layers: ellipses with aspect ratio approaching infinity. Based on principles of self consistent mechanics and the pure shear deformation of inclusions in a matrix, a direct expression is derived for the bulk viscosity of mixtures with orthogonal shape fabrics in pure shearing, in terms of the phase viscosity ratio, phase fractions, and a shape factor, p. The rheological properties of the mixtures are most usefully compared as normalised bulk viscosities with respect to the incompetent or competent phase (Figs. 4 and 5).

The 'relative horizontal distance', H, of Bons (1993), is verified by this modelling, and shown to be constant for mixtures of a particular geometry and p factor, regardless of the phase viscosity contrast (m) and phase fractions. The H value locates the bulk viscosity curve horizontally between the theoretical lower and upper viscous bounds for the two mixed phases. Circles mixtures occupy the half-way isotropic position ($H = 0.5$). For shape fabrics parallel/perpendicular to pure shearing, ellipses mixtures occupy the range from $H = 0.5$ to 1 (e.g. Fig. 7 upper half), increasing with ellipse ratio, R, demonstrating increasing bulk viscosity with stronger fabrics. Layered mixtures (ellipses with $R = \infty$) have the bulk viscosity of the upper viscous bound. Squares mixtures aligned in pure shear, if able to undergo heterogeneous clast strain, will behave more stiffly than circles mixtures, quite close to the upper bound ($H = 0.9$). On the other hand, rhombs mixtures would seem to behave as approximately circular and isotropic. The calculated bulk viscosities show increasing differences among mixtures with different shape fabrics, with increasing phase viscosity contrast, m (Figs. 4 and 5).

The symmetry of the graphical results allow some extrapolations to be made about circle/ellipse/layered mixtures oriented diagonally in pure shearing, as shown in Fig. 7. The mixtures that occupied the 'upper half' when aligned parallel to pure shearing, are suggested to occupy the 'lower half', when diagonally oriented, ranging from the central $H = 0.5$ curve for isotropic circles mixtures, progressively down towards the lower bound with increasingly elliptical diagonal fabrics, where the lower bound itself ($H = 0$) represents layers at 45° to pure shearing, or in layer-parallel simple shear. These diagonal two-phase mixtures in pure shear will therefore be less viscous than aligned mixtures with the same geometry.

The difference in the bulk viscosities of mixtures with orthogonal and diagonal shape fabrics in pure shearing, summarised in Fig. 7, can be used to quantify the anisotropy of the bulk viscosity. The results for pure shear can also be used to speculate on the rheology of the same mixtures in simple shear (Fig. 7), where the behaviour in simple shearing is 'equivalent' to pure shear rotated by 45°. Thus, the 'upper half' of the graph now represents circle/ellipse/layer mixtures with fabrics diagonal to simple shearing, and the 'lower half' depicts mixtures orthogonal to shearing.

Any conclusions for progressive deformation can only be tentative, because the modelling does not allow for difference in shape fabric of the two phases: and if there is a viscosity contrast, the two phases would be expected to deform by different rates, and so develop progressively different ellipticities. Qualitatively, however, the trend is likely to be an increasing mixture viscosity during progressive pure shear, for orthogonal shape fabrics with moderate phase viscosity contrasts. In simple shear, the progressive bulk behaviour could be more complex, and in a long-lived shearing system there might be cycles of stiffening and softening over time.

These two-dimensional results do not provide direct or accurate modelling of the three-dimensional bulk properties of two-phase viscous mixtures, but may arguably provide valid approximations for cross-sections. Differences emerge when comparing two and three dimensions (circles and spheres), arising from the different strain relationships in inclusion-matrix modelling for cylinders and spheres. However, it is argued that the inaccuracies of applying two-dimensional modelling to three-dimensional problems probably do not exceed those that surround any modelling of this kind that is based on statistical approximations and self-consistent mechanics. The two-dimensional analyses provide information on the interrelationships of bulk viscosity and mixture geometry that is not readily available from current three-dimensional methods.

Returning finally to conglomerates as an example of a geological mixture, the simplest of these might be modelled as a two-phase system comprising a single clast phase in a matrix with contrasting viscosity. It is concluded that the shapes and volume proportions of clasts will exert a strong control on the bulk properties of the rock, and on the degree of strain variation among the whole rock, the clast phase, and the matrix phase. These factors are being investigated in ongoing work on the deformation of conglomerates and other types of fragmental rocks.

Acknowledgements

This work has developed from joint work with Jack Treagus (NERC Grant GR3/10783) on deformed conglomerates, and was undertaken during the tenure of a NERC Senior Research Fellowship, both of which are gratefully acknowledged. Richard Hartley is thanked for drafting some of the figures. I appreciate receiving many constructive comments from Ray Fletcher, Win Means, Steve Covey-Crump, Paul Bons and Basil Tikoff, which together have helped in transforming earlier versions into this present paper.

References

Bilby, B.A., Kolbuszewski, M.L., 1977. The finite deformation of an inhomogeneity in two-dimensional slow viscous incompressible flow. Proceedings of the Royal Society A355, 335–353.

Bilby, B.A., Eshelby, J.D., Kundu, A.K., 1975. The change of shape of a viscous ellipsoidal region embedded in a slowly deforming matrix having a different viscosity. Tectonophysics 28, 265–274.

Biot, M.A., 1965. Mechanics of Incremental Deformations. John Wiley and Sons, New York.

Bloomfield, J.P., Covey-Crump, S.J., 1993. Correlating mechanical data with microstructural observations in deformation experiments on synthetic two-phase aggregates. Journal of Structural Geology 15, 1007–1019.

Bons, P.D., 1993. Experimental deformation of polyphase rock analogues. Ph.D. thesis, University of Utrecht, The Netherlands.

Bons, P.D., Cox, S.J.D., 1994. Analogue experiments and numerical modelling on the relation between microgeometry and flow properties of polyphase materials. Materials Science and Engineering A175, 237–245.

Budiansky, B., 1965. On the elastic moduli of some heterogeneous materials. Journal of the Mechanics and Physics of Solids 13, 223–227.

Cobbold, P.R., 1976. Mechanical effects of anisotropy during large finite deformations. Bulletin Societé Géologie France 7, 1497–1510.

Collyer, A.A., Clegg, D.W., 1988. Rheology Measurement. Elsevier Applied Science, London.

Einstein, A., 1906. Eine neue Bestimmung der Moleküldimension. Ann. Phys. Leipsig 19, 289–306.

Eshelby, J.D., 1957. The determination of the elastic field of an ellipsoidal inclusion, and related problems. Proceedings of the Royal Society A 241, 376–396.

Ferguson, J., Kemblowski, Z., 1991. Applied Fluid Rheology. Elsevier Applied Science, London.

Freeman, B., 1987. The behaviour of deformable ellipsoidal particles in three-dimensional slow flows: implications for geological strain analysis. Tectonophysics 132, 297–309.

Gay, N.C., 1968a. Pure shear and simple shear deformation of inhomogeneous viscous fluids. 1. Theory. Tectonophysics 5, 211–234.

Gay, N.C., 1968b. Pure shear and simple shear deformation of inhomogeneous viscous fluids. 2. The determination of the total finite strain in a rock from inclusions such as deformed pebbles. Tectonophysics 5, 295–302.

Ghosh, S.K., Ramberg, H., 1976. Reorientation of inclusions by combination of pure shear and simple shear. Tectonophysics 51, 83–97.

Handy, M.R., 1994. Flow laws for rocks containing two non-linear viscous phases: a phenomenological approach. Journal of Structural Geology 16, 287–301.

Hashin, Z., 1983. Analysis of composite materials — a survey. Journal of Applied Mechanics 50, 481–505.

Hill, R., 1965. A self-consistent mechanics of composite materials. Journal of the Mechanics and Physics of Solids 13, 213–222.

Hobbs, B.E., Means, W.D., Williams, P.F., 1976. An Outline of Structural Geology. John Wiley and Sons, New York.

Ji, S., Zhao, P., 1993. Flow laws of multiphase rocks calculated from experimental data on the constituent phases. Earth and Planetary Science Letters 117, 181–187.

Jordan, P., 1987. The deformational behaviour of bimineralic limestone–halite aggregates. Tectonophysics 135, 185–197.

Lisle, R.J., 1988. The superellipsoidal form of coarse clastic sediment particles. Mathematical Geology 20, 879–890.

Lisle, R.J., Rondeel, H.E., Doorn, D., Brugge, J., van de Gaag, P., 1983. Estimation of viscosity contrast and finite strain from deformed elliptical inclusions. Journal of Structural Geology 5, 603–609.

Mandal, N., Chakraborty, C., Samanta, S.K., 2000. An analysis of anisotropy of rocks containing shape fabrics of rigid inclusions. Journal of Structural Geology 22, 831–839.

Mckenzie, D., 1979. Finite deformation during fluid flow. Geophysical Journal of the Royal Astronomical Society 58, 689–715.

Shimamoto, T., 1975. The finite element analysis of the deformation of a viscous spherical body embedded in a viscous medium. Journal of the Geological Society of Japan 81, 255–267.

Takeda, Y.-T., 1998. Flow in rocks modelled as multiphase continua: application to polymineralic rocks. Journal of Structural Geology 20, 1569–1578.

Treagus, S.H., 1993. Flow variations in power-law multilayers: implications for competence contrasts in rocks. Journal of Structural Geology 15, 423–434.

Treagus, S.H., 1999. Are viscosity ratios measurable from cleavage refraction? Journal of Structural Geology 21, 895–901.

Treagus, S.H., Lan, L., 2000. Pure shear deformation of square inclusions, and applications to geological strain analysis. Journal of Structural Geology 21, 105–122.

Treagus, S.H., Treagus, J.E., 2001. Effects of object ellipticity on strain, and

implications for clast-matrix rocks. Journal of Structural Geology 23, 601–608.

Treagus, S.H., Hudleston, P.J., Lan, L., 1996. Non-ellipsoidal inclusions as geological strain markers and competence indicators. Journal of Structural Geology 18, 1167–1172.

Tullis, T.E., Horowitz, F.G., Tullis, J., 1991. Flow laws of polyphase aggregates from end-member flow laws. Journal of Geophysical Research 96, 8081–8096.